

ROBUST FEEDFORWARD CONTROL DESIGN FOR LATERAL VEHICLE
DYNAMICS

by

Semih TANKER

B.S., Mechanical Engineering, Boğaziçi University, 2008

Submitted to the Institute for Graduate Studies in
Science and Engineering in partial fulfillment of
the requirements for the degree of
Master of Science

Graduate Program in Mechanical Engineering

Boğaziçi University

2011

ACKNOWLEDGEMENTS

I would like to thank Prof. İ. Emre Köse for all the help and support. I feel lucky for being one of his students.

I would like to thank Prof. Eşref Eşkinat and Assoc. Prof. Tankut Acarman for participating in my thesis committee.

I would like to thank the assistants and colleagues at the Mechanical Engineering Department of Boğaziçi University.

Finally, I would like to thank my family for their support.

ABSTRACT

ROBUST FEEDFORWARD CONTROL DESIGN FOR LATERAL VEHICLE DYNAMICS

In this thesis, robust feedforward controller is designed for active steering which is an alternative vehicle dynamic control method to active braking control. The aim of this study is to increase performance and robustness of active steering using the combination of feedforward and feedback controller instead of using only feedback. A PID feedback controller is designed to stabilize a linear single track vehicle model with optimization of PID controller parameters. Feedforward controller is added to this controlled system to deal with uncertainties such as speed and cornering stiffness. Feedforward controller is designed using linear parameter varying (LPV) control theory and stability analysis results of integral quadratic constraints (IQCs). Both static and dynamic IQCs are used to describe uncertainty of the system and dual IQCs are used for stability analysis because of the nature of feedforward control problem. Linear matrix inequalities (LMIs) are used to define stability conditions. The controllers are designed such that the \mathcal{L}_2 -gain of the closed loop system is minimized. Simulation results of feedback controller, feedforward controller designed with static IQCs and feedforward controller designed with dynamic IQCs are given and compared for different steering angles.

ÖZET

YANAL ARAÇ DİNAMİĞİ İÇİN DAYANIKLI İLERİ BESLEMELİ KONTROL

Bu tezde, aktif fren denetimine alternatif bir taşıt dinamiği denetim yöntemi olan aktif yönlendirme için dayanıklı ileri beslemeli denetimci tasarlanmıştır. Bu çalışmanın amacı, sadece geri beslemeli denetimci kullanmak yerine, ileri ve geri beslemeli denetimcilerin kombinasyonunu kullanarak, aktif yönlendirmenin performansını ve dayanıklılığını arttırmaktır. PID denetimci parametrelerinin optimizasyonu ile doğrusal tek hatlı taşıt modelini kararlı duruma getirecek bir PID denetimci tasarlanmış ve bu denetlenmiş sisteme hız ve viraj alma sertlikleri gibi belirsizliklerle başa çıkması için ileri beslemeli denetimci eklenmiştir. İleri beslemeli denetimci sentezi için doğrusal parametreleri değişken (DPD) denetim teorisi ve integral kuadratik kısıtların (İKK) kararlılık analizi sonuçları kullanılmıştır. Sistemin belirsizliklerini ifade etmek için hem statik hem dinamik İKK'lar kullanılmıştır ve ileri beslemeli denetimcinin tabiatı gereği, analiz için eş İKK'lar kullanılmıştır. Kararlı duruma getirme koşullarını ifade etmek için doğrusal matris eşitsizlikleri kullanılmıştır. Denetimci, sistemin \mathcal{L}_2 kazancını en aza indirecek şekilde tasarlanmıştır. Geri beslemeli denetimcinin, statik İKK'lar ile tasarlanan ileri beslemeli denetimcinin ve dinamik İKK'lar ile tasarlanan ileri beslemeli denetimcinin farklı yönlendirme açıları için simülasyon sonuçları verilmiş ve karşılaştırılmıştır.

TABLE OF CONTENTS

ACKNOWLEDGEMENTS	iii
ABSTRACT	iv
ÖZET	v
LIST OF FIGURES	viii
LIST OF SYMBOLS	xi
LIST OF ACRONYMS/ABBREVIATIONS	xiii
1. NOTATION AND DEFINITIONS	1
2. INTRODUCTION	3
2.1. Stability Control of Vehicle	3
2.1.1. Active Braking Control	4
2.1.2. Active Differential System	5
2.1.3. Active Steering Control	6
2.1.4. Comparison of Active Steering and Braking	7
2.2. Control Methods for Active Steering	7
2.2.1. Feedback Control	8
2.2.2. Feedforward Control	9
2.2.3. Feedforward Control using IQCs	10
2.3. Organization of Thesis	11
3. LATERAL VEHICLE DYNAMICS AND CONTROL	12
3.1. Single Track Model	12
3.1.1. Relation Between Lateral Tire Force and Side Slip	13
3.1.2. Lateral Tire Forces	15
3.2. Feedback Control Design for Nominal Parameters	18
3.3. Uncontrolled Vehicle Response	20
3.4. Parametric Uncertainties in the Model	21
3.5. Uncertainty Representation in State-Space Descriptions	22
3.6. Robust Feedforward Control Synthesis	25
3.6.1. Performance Objective	27
4. CONVEX OPTIMIZATION AND LINEAR MATRIX INEQUALITIES	28

4.1. Convex Optimization	28
4.1.1. Local and Global Minima	28
4.2. Linear Matrix Inequalities	29
5. SYSTEM ANALYSIS VIA IQCs	32
5.1. Stability Analysis	32
5.2. Integral Quadratic Constraints	33
5.3. Robust Performance Problem	35
5.3.1. Dual IQCs	35
5.3.2. Dual IQCs in State-space	38
5.3.3. Selection of Multipliers	46
5.3.4. Generating LMIs for Static Multipliers	48
6. FEEDFORWARD CONTROLLER SYNTHESIS USING IQCS	52
6.1. Controller Synthesis	52
6.1.1. Selection of the Weighting Functions	52
6.1.2. Controller Synthesis with Static Multipliers	53
6.1.2.1. Static Design 1	53
6.1.2.2. Static Design 2	54
6.1.3. Controller Synthesis with Dynamic Multipliers	55
6.1.3.1. Dynamic Design 1	55
6.1.3.2. Dynamic Design 2	56
6.1.3.3. Dynamic Design 3	56
7. SIMULATIONS	58
7.1. Reference Values Corresponding to Drivers Steering Input	58
7.2. Lane Change Maneuver	59
7.3. Fishhook Maneuver	59
7.4. Simulation Results	60
8. CONCLUSIONS	68
REFERENCES	70

LIST OF FIGURES

Figure 2.1.	Yaw Stability Control System	4
Figure 2.2.	Active differential system	5
Figure 2.3.	ESP in 4 wheel drive	6
Figure 2.4.	Integral feedback active steering control	6
Figure 2.5.	FB control of a system.	8
Figure 2.6.	FB control of an uncertain system.	9
Figure 2.7.	FB/FF control of an uncertain system.	10
Figure 3.1.	Single track model.	13
Figure 3.2.	Lateral tire force and slip angle relation for different roads	14
Figure 3.3.	Real lateral tire force and slip angle relation	14
Figure 3.4.	Slip angle of front tire.	15
Figure 3.5.	Slip angle of rear tire.	16
Figure 3.6.	FB control of nominal system.	19
Figure 3.7.	Performance of PID controller with nominal vehicle parameters.	20
Figure 3.8.	Fishhook manoeuver on low friction road.	20

Figure 3.9.	FB control of uncertain system.	21
Figure 3.10.	Performance of PID controller with uncertain vehicle parameters.	22
Figure 3.11.	Spring mass damper system.	22
Figure 3.12.	Uncertainty representation of a spring mass damper system.	24
Figure 3.13.	Uncertainty representation of G	24
Figure 3.14.	Closed loop system with uncertainty block.	25
Figure 3.15.	Feedforward and feedback controllers.	25
Figure 3.16.	Feedforward controller for \tilde{G}	26
Figure 3.17.	System in LFT form.	27
Figure 3.18.	G_{cl} and Δ in LFT form.	27
Figure 5.1.	Disturbed interconnection of G and Δ	32
Figure 5.2.	Interconnection of G and Δ	33
Figure 5.3.	Performance of a system G	34
Figure 6.1.	System interconnection for FF controller design.	52
Figure 6.2.	Step response of system with static design 1.	54
Figure 6.3.	Step response of system with static design 2.	54

Figure 6.4.	Step response of system with dynamic design 1.	55
Figure 6.5.	Step response of system with dynamic design 2.	56
Figure 6.6.	Step response of system with dynamic design 3.	57
Figure 7.1.	Steering angle of lane change maneuver	59
Figure 7.2.	Fishhook maneuver steering wheel angle	60
Figure 7.3.	Response of vehicle with FB controller.	60
Figure 7.4.	Response of vehicle with FB/FF controller designed with static IQCs.	61
Figure 7.5.	Response of vehicle with FB/FF controller designed with dynamic IQCs.	61
Figure 7.6.	Sinusoidal steering input for $v = 36km/h$	62
Figure 7.7.	Sinusoidal steering input for $v = 72km/h$	63
Figure 7.8.	Sinusoidal steering input for $v = 108km/h$	63
Figure 7.9.	Random steering input with 1 degree mean for $v = 36km/h$	64
Figure 7.10.	Random steering input with 1 degree mean for $v = 72km/h$	64
Figure 7.11.	Random steering input with 1 degree mean for $v = 108km/h$	65
Figure 7.12.	Fishhook maneuver for $v = 108km/h$	66
Figure 7.13.	Real steering angle data for $v = 172km/h$ average.	67

LIST OF SYMBOLS

A, A_c	State matrices
a_y	Lateral acceleration
B, B_c, B_p, B_u, B_w	Input matrices
C, C_c, C_q, C_y, C_z	Output matrices
c_F	Cornering stiffness of front axle
c_R	Cornering stiffness of rear axle
C_{fb}	Feedback controller
C_{ff}	Feedforward controller
$C_{\alpha f}$	Cornering stiffness of front wheels
$C_{\alpha r}$	Cornering stiffness of rear wheels
D, D_c	Direct feedthrough matrices
D_{qp}, D_{qw}, D_{qu}	Direct feedthrough matrices
D_{zp}, D_{zw}, D_{zu}	Direct feedthrough matrices
e_β	Error of slip angle
$e_{\dot{\psi}}$	Error of yaw rate
F_{yf}	Lateral tire force on front axle
F_{yr}	Lateral tire force on rear axle
G	Model of vehicle
\tilde{G}	Model of vehicle controlled with feedback
J_z	Vehicle mass moment of inertia
k_d	Derivative coefficient
k_i	Integrator coefficient
k_p	Proportional coefficient
L_F	Distance from front axle to vehicle center of gravity
L_R	Distance from rear axle to vehicle center of gravity
M	Multiplier for the dual IQC
\mathcal{P}	Internal Supply Rates
u_{fb}	Output of feedback controller
u_{ff}	Output of feedforward controller

V	Speed of vehicle
w	Disturbance input
W_e	The weighting function for the error
W_r	The weighting function for the reference signal
x	State vector
y	Measured output
z	Controlled output
α	Tire slip angle
β	Slip angle
δ	Wheel angle
δ_c	Wheel angle correction
δ_k	Uncertainty of parameter
Δ	Uncertainty block
μ	Road adhesion factor
Π	Multiplier for the primal IQC
θ_{V_f}	Front wheel velocity angle
θ_{V_r}	Rear wheel velocity angle
ψ	Yaw angle

LIST OF ACRONYMS/ABBREVIATIONS

ABS	Anti-lock Braking System
ESP	Electronic Stability Program
FB	Feedback
FF	Feedforward
IQC	Integral Quadratic Constraints
LFT	Linear Fractional Transformation
LMI	Linear Matrix Inequality
LPV	Linear Parameter Varying
VDC	Vehicle Dynamic Control

1. NOTATION AND DEFINITIONS

Realization of a state space system is represented as $G(s) = \left[\begin{array}{c|c} A & B \\ \hline C & D \end{array} \right]$ where $G(s) = C(sI - A)^{-1}B + D$ and state space system is

$$\dot{x} = Ax + Bu \quad (1.1)$$

$$y = Cx + Du. \quad (1.2)$$

We use the notation $M \succ 0$ where M is 'positive definite' and $M \succeq 0$ where M is 'positive semi-definite'.

Definition 1.1. (\mathcal{L}_p Space) For $p \in [1, \infty)$, the \mathcal{L}_p space is defined as

$$\mathcal{L}_p[0, \infty) := \left\{ x : \text{Lebesgue - measurable} \mid \int_0^\infty |x(t)|^p dt < \infty \right\}. \quad (1.3)$$

The space of matrix-valued functions with entries that are essentially bounded on the imaginary axis is denoted by \mathcal{L}_∞ . For two signals $a, b \in \mathcal{L}_2^n$, the inner product of $\langle a, b \rangle$ is defined as

$$\langle a, b \rangle := \frac{1}{2\pi} \int_{-\infty}^{\infty} \hat{a}(j\omega)^* \hat{b}(j\omega) d\omega \quad (1.4)$$

where \hat{a} and \hat{b} are Fourier transforms of a and b . The Fourier transform of $a \in \mathcal{L}_2^n$ is

$$\hat{a}(j\omega) := \int_0^\infty e^{-j\omega t} a(t) dt \quad (1.5)$$

Then, \mathcal{L}_2 norm of a is defined as $\|a\|_2 := \langle a, a \rangle^{1/2}$ and induced \mathcal{L}_2 norm of system G is

$$\|G\|_{i_2} := \sup_{w \in \mathcal{L}_2, w \neq 0} \frac{\|Gw\|_2}{\|w\|_2}. \quad (1.6)$$

If $\|G\|_{i_2}$ is finite, then G is "bounded".

Definition 1.2. (Inertia) Given a $\Pi = \Pi^T \in \mathbb{R}^{n \times n}$, its inertia is $in(\Pi) = (n_+, n_-, n_0)$ where n_+ is number of positive eigenvalues of Π , n_- is number of negative eigenvalues of Π and n_0 is number of zero eigenvalues of Π .

Definition 1.3. Let $S \in \mathbb{R}^{n \times m}$ be a full column-rank matrix. $S_\perp \in \mathbb{R}^{n \times (n-m)}$ denotes any matrix whose columns form a basis for the kernel of S^T , that is, $S^T S_\perp = 0$ and $\begin{pmatrix} S & S_\perp \end{pmatrix}$ is invertible.

E.g. If $S = \begin{pmatrix} M \\ I \end{pmatrix} \Rightarrow S_\perp = \begin{pmatrix} I \\ -M^T \end{pmatrix}$

In certain places, we use \star instead of writing the content where the content of a matrix is obvious.

2. INTRODUCTION

In this study, robust feedforward controller is designed for lateral vehicle dynamic control. Active steering is studied as an alternative for electronic stability control. Feedforward controller is designed and used with feedback controller to improve robustness and performance since the feedback controller cannot show sufficient tracking performance even for small changes of uncertain parameters.

In the last few decades, development in computer and electronics, and also lower prices of a control system make it possible to apply a control system for vehicles for safety and comfort [1]. Most of the accidents with injuries caused by losing control of vehicle and spinning cars. These accidents are mostly caused by overreaction of drivers. Different vehicle dynamics control (VDC) methods are used in the industry such as anti-lock braking system (ABS), active braking control (Bosch's ESP) [2] and active steering control [3] to improve vehicle handling in extreme cases.

2.1. Stability Control of Vehicle

The purpose of stability control is improving vehicle handling and decreasing the possibility of spinning. Panic and overreaction of unexperienced drivers result with losing control of vehicle in extreme cases. Lower prices of piezoelectric sensors and development in computer technologies make possible to produce vehicles which can sense such an occasion and prevent an accident.

The function of stability control can be seen in Figure (2.1). The aim of stability control is keep slip angle as low as possible while tracking a yaw rate as seen in middle curve even driving in low friction roads. Maximum limit of slip angle is 8° in dry roads and 2° in wet roads. Even if we are driving in high friction roads, oversteering can increase slip angle over the maximum limit and cause spinning of vehicle [1, 4].

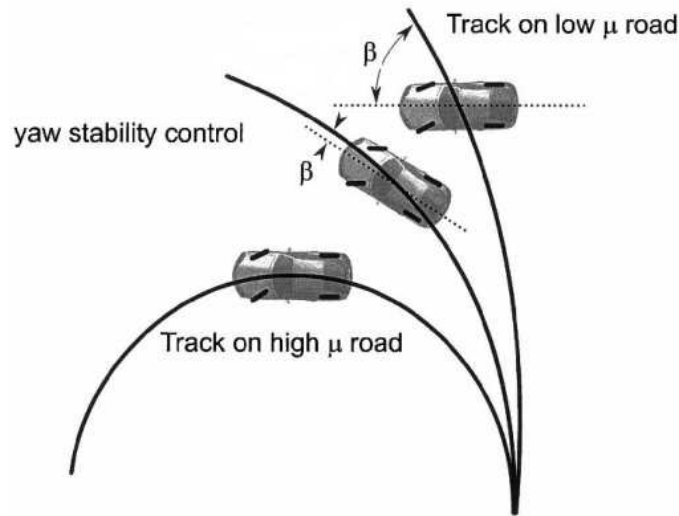


Figure 2.1. Yaw stability control system [1].

Electronic Stability Program (ESP) is one of the widely used method to improve stability of vehicle by correcting panic reactions of unexperienced drivers [2]. Purpose of ESP is to improve vehicle handling by controlling brakes and engine torque. Required yaw moment is created by controlling individual wheel brake. Anti-lock braking system (ABS) is used as actuator of ESP and some of the required sensors are already exists on ABS. Since most of the components already exist on the vehicle, ESP require less hardware to be applied on vehicle. That is why it is widely used in industry.

Even if new generation of stability control methods use more than one actuator, it is possible to classify stability control methods according to their actuators such as:

- Active Braking Control
- Active Steering Control
- Active Differential Systems

2.1.1. Active Braking Control

First generation ESP of Bosch is actually an active braking system. Required yaw rate is derived from the approximation of the vehicle measurements using single track model of the vehicle. Required yaw moment to stabilize the vehicle is achieved by

controlling individual wheel brakes. ESP is using ABS in this purpose. Components of ESP are wheel speed sensors, steering wheel angle sensor, yaw rate sensor and a control unit. Since components of ESP is already exist is a vehicle, it can be considered as more applicable.

New ESP systems applied to 4 wheel drive systems can be considered as a hybrid of active braking and active differential which we explain in the following section.

2.1.2. Active Differential System

If braking used to create a stabilizing yaw moment, longitudinal acceleration of the vehicle is decreased in contradiction with driver needs. Active torque distribution system can achieve stability by controlling torque transferred to each wheel [1].

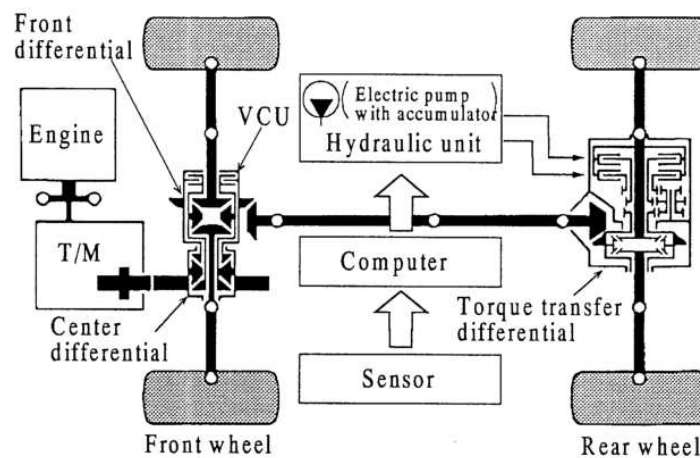


Figure 2.2. Active differential system [5].

In [5], a differential is introduced in which torque can be transferred to each wheel separately. Both yaw stability and traction control can be achieved by using such a differential with a control system calculating required yaw moment and torques for each wheel.

Adaptation of ESP to 4 wheel drive explained in [6]. It is combination of active braking and active differential. Basically, controller calculate the required yaw moment

for stability same as the standard ESP. But actuators of creating this yaw moment are both brakes and differentials as shown in Figure (2.3). Idea of using existing hardware also make this new approach applicable for both ease and commercial reasons.

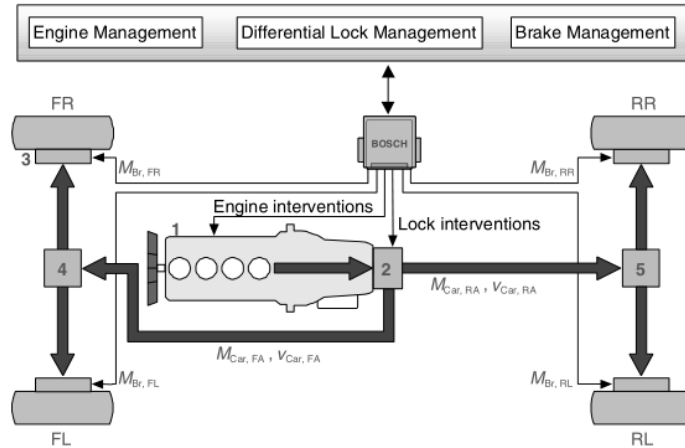


Figure 2.3. ESP in 4 wheel drive [6].

2.1.3. Active Steering Control

Active steering systems improve vehicle handling with small modifications of steering angle given by driver. Desired yaw rate is also determined using single track model of vehicle depending on driver's steering input. Yaw rate of vehicle is also measured by yaw rate sensors. Steering angle is modified by a feedback controller depending on the difference between reference and measured yaw rates. Ackermann introduced this in 1996.

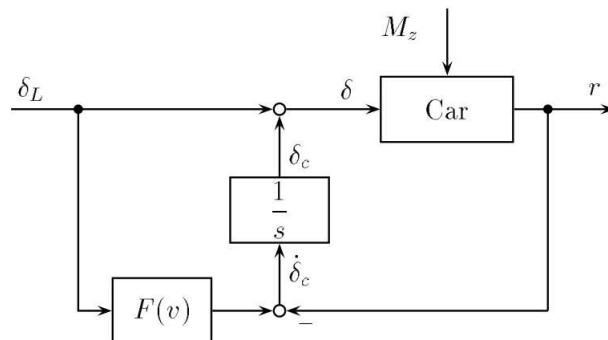


Figure 2.4. Integral feedback active steering control [3].

In [3] a robust active steering control is introduced to improve vehicle handling. A small correction is added to steering angle given by driver. This correction is obtained by integral feedback of yaw rate error which is obtained from the difference between driver commanded yaw rate and measured yaw rate of vehicle. Since steering angle has direct effect on yaw dynamic, it is more effective. But active steering requires more hardware to create correction on steering angle.

2.1.4. Comparison of Active Steering and Braking

In active braking and active torque systems such as ESP, stabilizing yaw moment created by distributing braking force and engine torque on each wheel depending on difference between desired and measured yaw rate values. Active steering is more efficient with direct effect on vehicle yaw dynamic and more robust in different road characteristics and whether conditions considering physical limitations of individual braking such as friction between tires and slippery roads. Active braking system required less additional hardware since actuator and sensors already exist in ABS.

Active steering can be an alternative for ESP as well as they can be used together. We study active steering considering direct effects of steering angle on yaw dynamics. It is possible to design more robust controller with active steering than the one with active braking since uncertainties of cornering stiffness affect tracking response of vehicle. Stabilizing yaw moment directly depend on friction between tires and road in active braking control. On a low μ road vehicle become less stable when stabilizing actuation of individual braking is less effective.

2.2. Control Methods for Active Steering

Different control methods can be used for active steering. As discussed in [7] robust feedforward controller can be designed or a robust feedforward controller can be used with stabilizing feedback controller as discussed in [8]. We give introduction to both feedback control and feedforward control.

2.2.1. Feedback Control

As discussed in [3] it is possible to control stability of vehicle using a feedback controller. As shown in Figure (2.4), feedback controller give a correction to drivers steering angle by evaluating the difference between the desired yaw rate and actual yaw rate measured. In this study, we considered output of controller is actuated by a steer by wire system and our controller create directly a steering angle which is corrected driver input. We design a feedback controller such as:

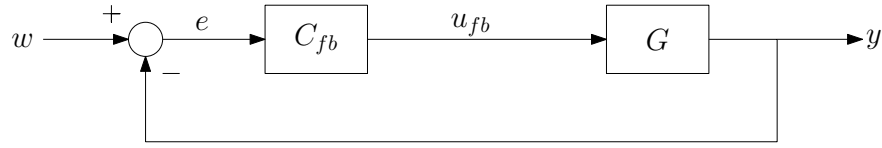


Figure 2.5. FB control of a system.

where G is vehicle model, $w = \begin{pmatrix} \beta_{ref} \\ \dot{\psi}_{ref} \end{pmatrix}$, $e = \begin{pmatrix} e_{\beta} \\ e_{\dot{\psi}} \end{pmatrix}$ and C_{fb} is feedback controller such as

$$C_{fb}(s) = \begin{bmatrix} K_{\beta}(s) & K_{\dot{\psi}}(s) \end{bmatrix} \quad (2.1)$$

where $K_{\beta}(s)$ and $K_{\dot{\psi}}(s)$ are PID approximates such that

$$K_{\beta}(s) = k_{p\beta} + \frac{k_{i\beta}}{s} + \frac{k_{d\beta}s}{0.001s + 1} \quad (2.2)$$

and

$$K_{\dot{\psi}}(s) = k_{p\dot{\psi}} + \frac{k_{i\dot{\psi}}}{s} + \frac{k_{d\dot{\psi}}s}{0.001s + 1}. \quad (2.3)$$

Controller parameters are designed with parameter optimization for reference tracking. The optimization is performed for nominal values of vehicle parameter. Tracking performance is satisfactory for nominal values. But for a system with uncertainties, tracking performance decrease. It is possible represent uncertainties with a Δ such as;

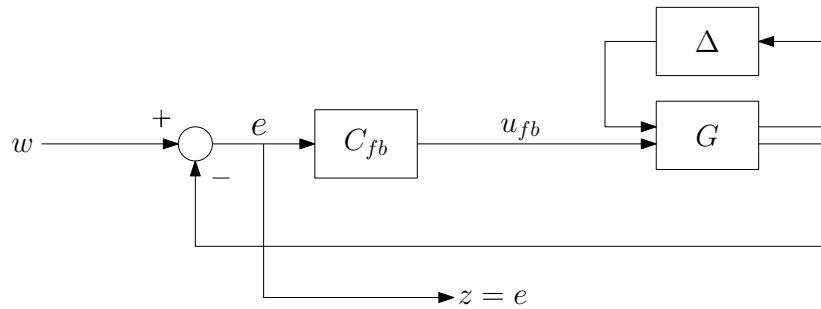


Figure 2.6. FB control of an uncertain system.

where $\Delta = \text{diag}(\delta_1 I_{n_1}, \delta_2 I_{n_2}, \dots, \delta_k I_{n_k})$, k present number of uncertain parameters, n_k is size of each uncertainty channel and $\|\delta_i\| \leq 1 \quad \forall i = 1 : k$. Feedback controller cannot deal with this uncertainties well. So we propose the use of feedforward controller to deal with Δ .

2.2.2. Feedforward Control

An active steering method using combination of feedback and feedforward controllers is developed in [8] to improve vehicle handling. Uncertain parameters are considered and it is seen that vehicle stability, performance and robustness are improved for different type of maneuvers.

The combination of FF and FB is widely used in industry. FB is generally used to stabilize the system and FF is used to increase tracking performance of the system. Use of FB alone is not sufficient for a system with uncertain parameters such as different road characteristics, mass and speed of vehicle. Even if tracking performance of feedback control applied to vehicle dynamics is satisfactory for nominal values of vehicle parameters, setting time and fluctuations of tracking response is increasing with small changes in uncertain parameters.

The model of FB/FF control of an uncertain system is shown in Figure (2.7). It is seen that system became more robust to uncertainties and tracking performance is also increased if we add a feedforward controller to a system which is already controlled

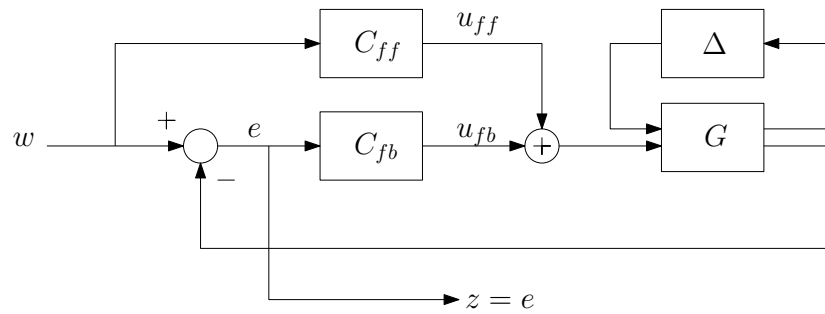


Figure 2.7. FB/FF control of an uncertain system.

with feedback controller. In this study, feedforward controller is designed with Integral Quadratic Constraints (IQCs) involving both static and dynamic multiplier to improve both performance and robustness.

2.2.3. Feedforward Control using IQCs

IQCs which is used in this thesis is discussed in [9]. In [10], IQC for channel w to z is used to increase performance of an LPV (Linear Parameter Varying) system. Use of full block static multipliers is formulated in [10] and it differs from the forms constructed in [9]. Both methods are used and compared in this thesis.

A finite dimensional, convex solution to the problem of robust \mathcal{L}_2 -gain feedforward control design is given in [11]. Dynamic multipliers is used to describe the uncertainties. A feedforward controller is designed by application of dual formulation to the system. FB/FF results are compared with FB and it is seen that settling time is reduced and overshoot is minimized.

A new method is explained in [12] to design a feedforward controller for electromechanical servo systems. The aim of the study is to minimize the settling time. The proposed method is applied to wafer stage and settling time can be reduced comparison to the existing methods in simulations even if zero-settling is not achieved in experiments.

Output-tracking performance of the use of the inversion based feedforward input

and the use of feedback alone is compared in [13]. It is seen that inverse-based feedforward controller improves the output-tracking performance at frequencies where the the uncertainty in nominal plant is smaller than the rate of the size of the plant and its condition number.

In this thesis we focus on only active steering control and we use combination of feedback and feedforward control as in Figure 2.7 and make robust \mathcal{L}_2 -gain feedforward controller design to increase performance and robustness of classic feedback control. We use both static and dynamic IQCs for feedforward controller synthesis.

2.3. Organization of Thesis

In Chapter 3, equation of motions of a vehicle is derived, feedback controller designed for nominal vehicle model and compared with uncertain vehicle model. Feedforward controller added to this closed loop feedback controlled system to improve robustness to this uncertainties. In Chapter 4, general information are given about convex optimization and linear matrix inequalities (LMIs). In Chapter 5, integral quadratic constraints are explained and general information are given about controller design using IQCs. In Chapter 6, feedforward controller is designed using the methods introduced. In Chapter 7, simulation of the vehicle model are performed for specific inputs using the controllers designed in Chapter 6 and they are compared with simulations using FB only. In Chapter 8, conclusions and summary of the main contributions are given and recommendations for further work are also included.

3. LATERAL VEHICLE DYNAMICS AND CONTROL

In this chapter, basic information is given about lateral vehicle dynamic and feedback control of vehicle using active steering is introduced. First, single track model or bicycle model is shown. Since bicycle model is linear single track model, validation of this model for our purpose is explained. This model is appropriate because we are considering the linear region of tire force behavior with small steering angle assumption in this study. After single track model put in state space form, we explain control of system with feedback active steering control.

3.1. Single Track Model

Single track model of a vehicle is introduced in this section. Single track model or bicycle model is a simple vehicle model but it is frequently used in studies about steering problem. Several assumptions are made. Left and right front wheels are assumed to have approximately equal steering angles. Left and right tires in each axle are combined in the centerline of vehicle. Since it has only two tires in this model, it is named as bicycle model. But it is not similar to handling of bicycle. Because bicycle make a vertical angle at corners. Aerodynamic forces are not considered and there is no suspension in the model we used. Tire model assumed to be linear with small angle approximation [14, 15, 16].

Equation of motion for a vehicle along the y axis is

$$ma_y = F_{yf} + F_{yr} \quad (3.1)$$

where a_y is acceleration of vehicle in y axis and F_{yf} and F_{yr} are lateral tire forces. a_y is combination of \ddot{y} and centripetal acceleration.

$$a_y = \ddot{y} + V_x \dot{\psi} \quad (3.2)$$

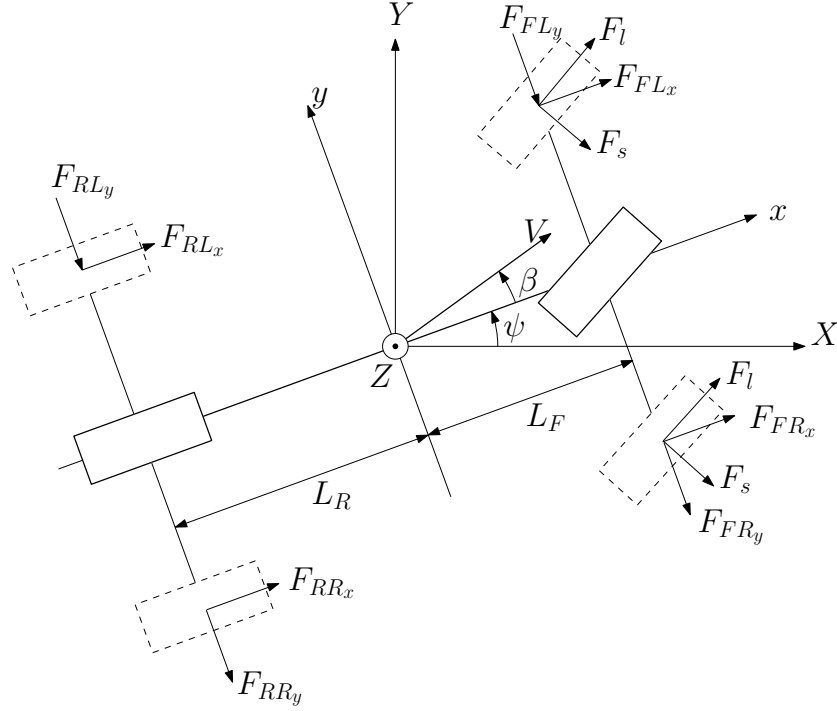


Figure 3.1. Single track model.

if 3.2 is substituted into 3.1,

$$m \left(\ddot{y} + V_x \dot{\psi} \right) = F_{yf} + F_{yr} \quad (3.3)$$

Moment balance in z-axis is

$$J_z \ddot{\psi} = L_F F_{yf} - L_R F_{yr} \quad (3.4)$$

3.1.1. Relation Between Lateral Tire Force and Side Slip

Lateral forces and friction between tire and road are important for vehicle safety improvement and designing controller for better handling. For higher slip angles estimation of lateral tire force is more complex since tire behavior is nonlinear [15]. But for smaller angles lateral tire force is proportional to slip angle and can be assumed linear as seen in Figure 3.2. This proportionality constant is cornering stiffness.

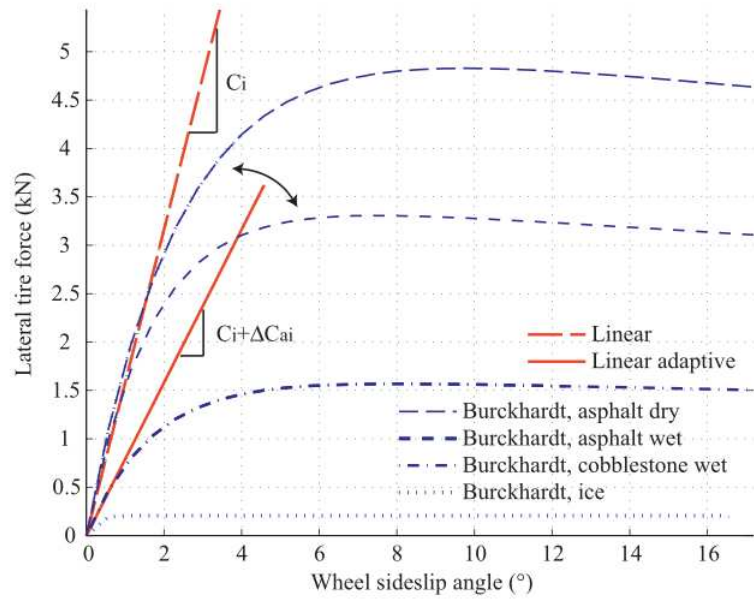


Figure 3.2. Lateral tire force and slip angle relation for different roads [17].

We can make small angle assumption for vehicle handling and stability improvements using active steering since we are trying to minimize slip angle while tracking the required yaw rate. We apply maximum limit of $\beta_{max} = 2^\circ$ for side slip in order to make valid assumption and it is a limit for spinning in slippery roads.

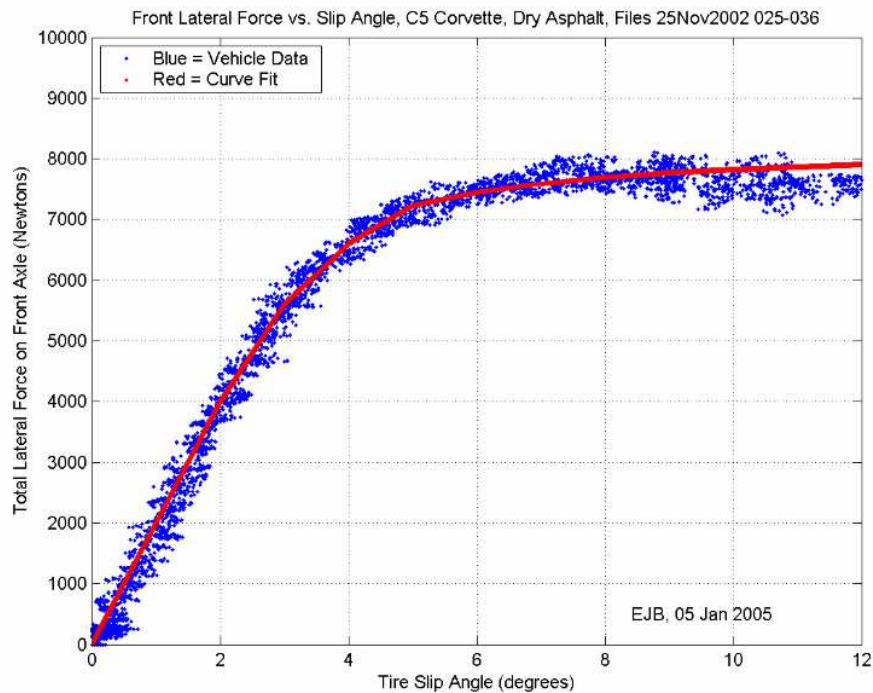


Figure 3.3. Real lateral tire force and slip angle relation [18].

A real lateral force and slip angle relation is also shown in Figure 3.3. Lateral tire forces depend primarily on the tire slip angle and surface coefficient of adhesion as specified in [18]. Lateral tire force and slip angle relation is almost linear up to 2° as seen in Figure 3.3.

3.1.2. Lateral Tire Forces

Lateral tire forces is proportional to slip angle of tires for small angles as discussed in previous section. Slip angle of tire is the angle between direction of the tire and angle of velocity vector. Following figure represent front tire.

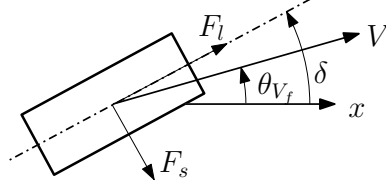


Figure 3.4. Slip angle of front tire.

The slip angle of front wheel is

$$\alpha_f = \delta - \theta_{V_f} \quad (3.5)$$

Then side forces on front tires are

$$F_s \cong C_{\alpha_f} (\delta - \theta_{V_f}) \quad (3.6)$$

Lateral forces on front tires are components of F_s and F_l in y direction

$$F_{FL_y} \cong F_{FR_y} \cong F_s \cos(\delta) + F_l \sin(\delta) \quad (3.7)$$

With the assumption of $\sin(\delta) \cong 0$ and $\cos(\delta) \cong 1$, lateral forces on front tires are

$$F_{FL_y} \cong F_{FR_y} \cong C_{\alpha_f} (\delta - \theta_{V_f}) \quad (3.8)$$

Following figure show slip angle of rear tire.

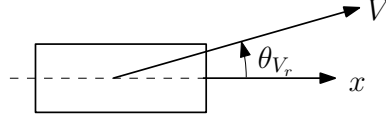


Figure 3.5. Slip angle of rear tire.

Since steering angle of rear wheel is zero, the slip angle of rear wheel is

$$\alpha_r = -\theta_{V_r} \quad (3.9)$$

Then lateral forces on rear tires are

$$F_{RL_y} \cong F_{RR_y} \cong C_{\alpha_r} (-\theta_{V_r}) \quad (3.10)$$

Since there is left and right tires assumed to be placed on centerline, we add lateral forces of front tires up, then lateral force on front axle will be

$$F_{yf} = F_{FL_y} + F_{FR_y} \quad (3.11)$$

F_{FL_y} and F_{FR_y} are assumed to be equal, then

$$F_{yf} \cong 2C_{\alpha_f} (\delta - \theta_{V_f}) \quad (3.12)$$

If lateral forces of rear tires are added up, then lateral force on rear axle will be

$$F_{yr} = F_{RL_y} + F_{RR_y} \quad (3.13)$$

F_{RL_y} and F_{RR_y} are assumed to be equal, then

$$F_{yr} \cong 2C_{\alpha_r} (-\theta_{V_r}) \quad (3.14)$$

where C_{α_f} and C_{α_r} are cornering stiffness of front and rear wheels respectively. $2C_{\alpha_f}$ and $2C_{\alpha_r}$ is used since we combine properties of left and right tires at the centerline of vehicle. Velocity angle of front tire can be approximated by

$$\tan(\theta_{V_f}) \cong \frac{V_y + L_F \dot{\psi}}{V_x} \quad (3.15)$$

and velocity angle of rear tire can be approximated by

$$\tan(\theta_{V_r}) \cong \frac{V_y - L_R \dot{\psi}}{V_x} \quad (3.16)$$

Let use notation \dot{y} for V_y instead then velocity angles with small angle approximation

$$\theta_{V_f} \cong \frac{\dot{y} + L_F \dot{\psi}}{V_x} \quad (3.17)$$

$$\theta_{V_r} \cong \frac{\dot{y} - L_R \dot{\psi}}{V_x} \quad (3.18)$$

Substitute 3.12, 3.14, 3.17, 3.18 into 3.3 and 3.4

$$m \left(\ddot{y} + V_x \dot{\psi} \right) = 2C_{\alpha_f} \left(\delta - \frac{\dot{y} + L_F \dot{\psi}}{V_x} \right) + 2C_{\alpha_r} \left(\frac{-\dot{y} + L_R \dot{\psi}}{V_x} \right) \quad (3.19)$$

$$J_z \ddot{\psi} = 2L_F C_{\alpha_f} \left(\delta - \frac{\dot{y} + L_F \dot{\psi}}{V_x} \right) - 2L_R C_{\alpha_r} \left(\frac{-\dot{y} + L_R \dot{\psi}}{V_x} \right) \quad (3.20)$$

If we replace $\dot{y} = \beta V_x$, $2C_{\alpha_f} = C_F$, $2C_{\alpha_r} = C_R$, $V_x = v$, we obtain simplified equation of motion of vehicle, which are

$$mv \left(\dot{\beta} + \dot{\psi} \right) = c_F \left(\delta_W - \beta - \frac{L_F \dot{\psi}}{v} \right) + c_R \left(-\beta - \frac{L_R \dot{\psi}}{v} \right) \quad (3.21)$$

$$J_z \ddot{\psi} = c_F L_F \left(\delta_W - \beta - \frac{L_F \dot{\psi}}{v} \right) + c_R L_R \left(-\beta - \frac{L_R \dot{\psi}}{v} \right) \quad (3.22)$$

We can easily write above equations in state space form such as:

$$\dot{x} = \begin{bmatrix} -\frac{c_F + c_R}{mv} & \frac{c_R L_R}{mv^2} - \frac{c_F L_F}{mv^2} - 1 \\ \frac{c_R L_R - c_F L_F}{J_z} & -\frac{c_F L_F^2 + c_R L_R^2}{J_z v} \end{bmatrix} x + \begin{bmatrix} \frac{c_F}{mv} \\ \frac{c_F L_F}{J_z} \end{bmatrix} \delta_w \quad (3.23)$$

$$y = \begin{bmatrix} 1 & 0 \\ 0 & 1 \end{bmatrix} x$$

where state matrix is

$$x = \begin{pmatrix} \beta \\ \dot{\psi} \end{pmatrix}, \quad \dot{x} = \begin{pmatrix} \dot{\beta} \\ \ddot{\psi} \end{pmatrix} \quad (3.24)$$

We obtain a state space model of vehicle for small tire angles. Since our tire model is linear with small angle approximation, this model won't be valid for large tire angles. Because tire model is not linear at large angles. Since we use this model model with small wheel angles given by driver and our controller give small correction angles, it is valid for our purposes.

3.2. Feedback Control Design for Nominal Parameters

In this section, we design feedback controllers for yaw rate tracking of the vehicle model derived above. Feedback controller is designed to stabilize the nominal system. G_{nom} is the system 3.23 with nominal values of vehicle parameters c_R , c_F , L_F , L_R , m , v and J_z such that

$$m = 1573kg \qquad I_z = 2873kgm^2 \quad (3.25)$$

$$L_F = 1.1m \qquad L_R = 1.58m \qquad (3.26)$$

$$C_{\alpha f} = 80000N/rad \qquad C_{\alpha r} = 80000N/rad \qquad (3.27)$$

$$v = 72km/h. \qquad (3.28)$$

We can see the feedback controller of the nominal system in Figure 3.6.

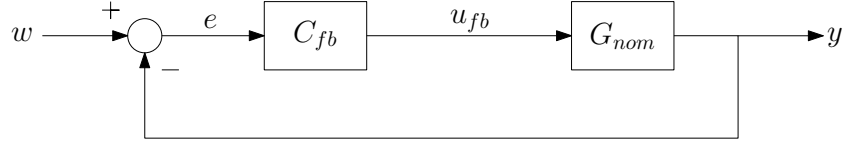


Figure 3.6. FB control of nominal system.

where

$$w = \begin{pmatrix} \beta_{ref} \\ \dot{\psi}_{ref} \end{pmatrix}, \quad e = \begin{pmatrix} e_{\beta} \\ e_{\dot{\psi}} \end{pmatrix}, \quad u_{fb} = \delta_w \qquad (3.29)$$

Feedback controller is in the form of:

$$C_{fb}(s) = \begin{bmatrix} K_{\beta}(s) & K_{\dot{\psi}}(s) \end{bmatrix} \qquad (3.30)$$

where $K_{\beta}(s)$ and $K_{\dot{\psi}}(s)$ are PID approximates such that

$$K_{\beta}(s) = k_{p\beta} + \frac{k_{i\beta}}{s} + \frac{k_{d\beta}s}{0.001s + 1} \qquad (3.31)$$

and

$$K_{\dot{\psi}}(s) = k_{p\dot{\psi}} + \frac{k_{i\dot{\psi}}}{s} + \frac{k_{d\dot{\psi}}s}{0.001s + 1}. \qquad (3.32)$$

PID controller is designed for this nominal system. We use parameter optimization method to optimize $k_{p\dot{\psi}}$, $k_{p\beta}$, $k_{i\dot{\psi}}$, $k_{i\beta}$, $k_{d\dot{\psi}}$ and $k_{d\beta}$ which are proportional, integral and derivative coefficients respectively.

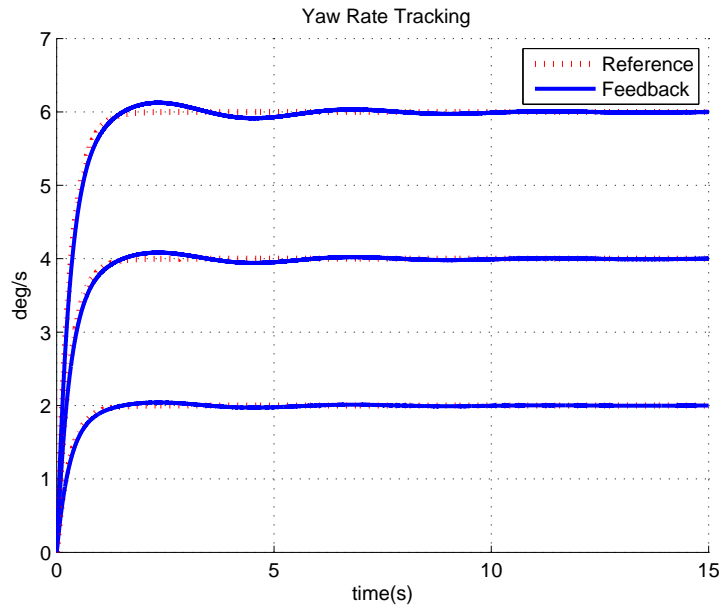


Figure 3.7. Performance of PID controller with nominal vehicle parameters.

3.3. Uncontrolled Vehicle Response

Before explain feedback and feedforward control of a vehicle it is helpful to give uncontrolled response of vehicle for a steering angle. We give yaw rate response of

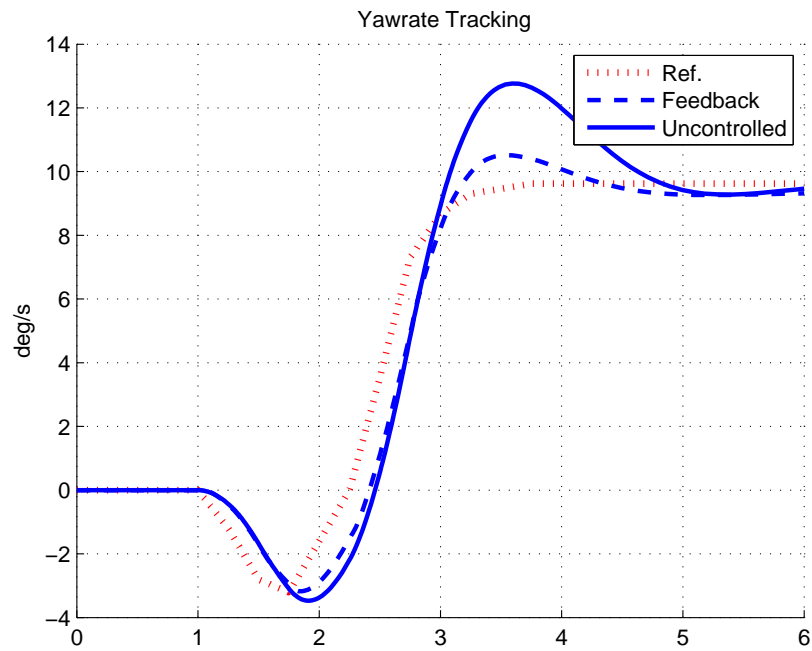


Figure 3.8. Fishhook manoeuver on low friction road.

fishhook manoeuver on low friction road in Figure 3.8. Speed of vehicle is 72km/h and cornering stiffness is 20kN/rad . Response of controlled system is also included to demonstrate aim of control. Desired yaw rate corresponding to drivers steering angle is steady state response of single track model. Reference yaw rate is given in (7.4).

3.4. Parametric Uncertainties in the Model

Feedback controllers performance is decreased with uncertain parameters of vehicle such as speed and cornering stiffness. G_{unc} is the system 3.23 where uncertain vehicle parameters such as c_R , c_F and v are

$$C_{\alpha_f} \in (40\text{kN/rad}, 80\text{kN/rad}) \quad C_{\alpha_r} \in (40\text{kN/rad}, 80\text{kN/rad}) \quad (3.33)$$

$$v \in (36\text{km/h}, 108\text{km/h}) \quad (3.34)$$

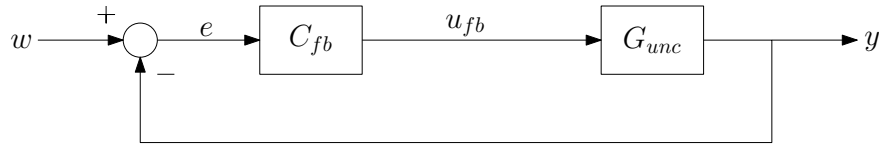


Figure 3.9. FB control of uncertain system.

We simulate our vehicle model controlled by feedback controller designed for nominal values and result is seen in Figure 3.10.

We can see in Figure 3.10, overshoot and settling time increasing while cornering stiffness is decreasing. We design our feedback controller for nominal values of parameters and when this parameters change during operation or before the operation, feedback controller stop working properly. Parameters such as cornering stiffness cannot be measured online and we want our controller be robust for this kind of changes.

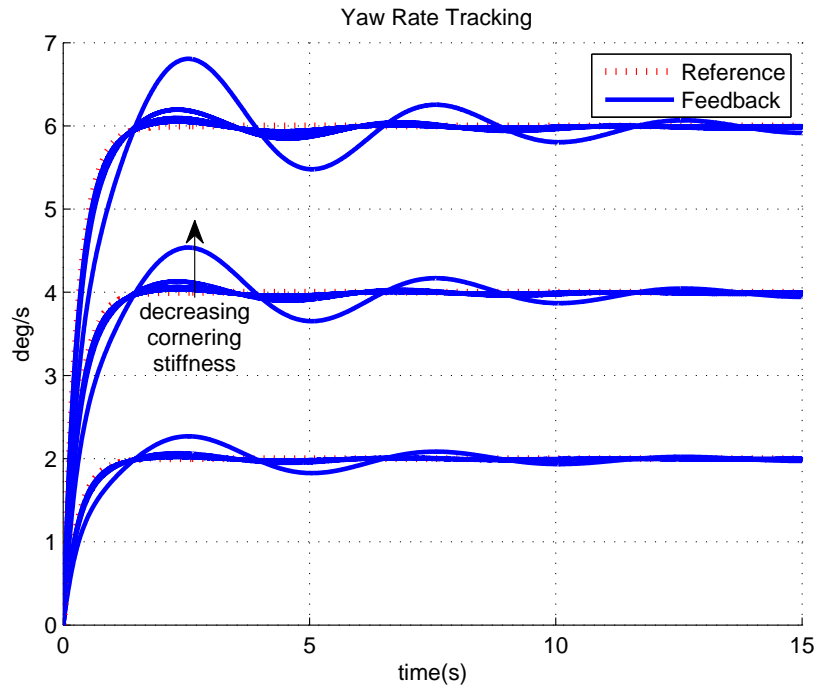


Figure 3.10. Performance of PID controller with uncertain vehicle parameters.

3.5. Uncertainty Representation in State-Space Descriptions

It is seen that uncertainties in a system affect performance and robustness of a system. If the system matrices are rational functions of parameters, we can express uncertainties in a block matrix Δ . Before explain form of Δ , a simple example is given to explain uncertainties clearly.

Example: Consider a spring mass damper system with uncertainty in k as in Figure 3.11.

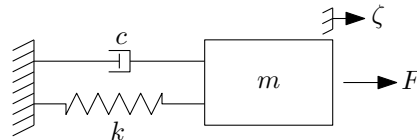


Figure 3.11. Spring mass damper system.

Equation of motion of such a system is

$$m\ddot{\zeta} + c\dot{\zeta} + k\zeta = F \quad (3.35)$$

Suppose $k = k_0(1 + k^*\delta_k)$ where $|\delta_k| \leq 1$. Then,

$$m\ddot{\zeta} + c\dot{\zeta} + k_0\zeta + k_0k^*\delta_k\zeta = F \quad (3.36)$$

$$\Leftrightarrow m\ddot{\zeta} + c\dot{\zeta} + k_0\zeta = F - k_0k^*\delta_k\zeta \quad (3.37)$$

Let $q := \zeta$ and $p := \delta_k\zeta$. If $\Delta := \delta_k$ and $p = \Delta q$ then

$$m\ddot{\zeta} + c\dot{\zeta} + k_0\zeta = F - k_0k^*p \quad (3.38)$$

Then, it can be written as

$$\dot{x} = \begin{pmatrix} 0 & 1 \\ \frac{-k_0}{m} & \frac{-c}{m} \end{pmatrix} \begin{pmatrix} \zeta \\ \dot{\zeta} \end{pmatrix} + \begin{pmatrix} 0 \\ \frac{-k_0k^*}{m} \end{pmatrix} p + \begin{pmatrix} 0 \\ \frac{1}{m} \end{pmatrix} F \quad (3.39a)$$

$$q = \begin{pmatrix} 1 & 0 \end{pmatrix} \begin{pmatrix} \zeta \\ \dot{\zeta} \end{pmatrix} \quad (3.39b)$$

$$y = \begin{pmatrix} 1 & 0 \end{pmatrix} \begin{pmatrix} \zeta \\ \dot{\zeta} \end{pmatrix} \quad (3.39c)$$

which is equivalent to

$$\begin{pmatrix} q \\ y \end{pmatrix} = \left[\begin{array}{c|cc} A & B_p & B_u \\ \hline C_q & D_{qp} & D_{qu} \\ C_y & D_{yp} & D_{yu} \end{array} \right] \begin{pmatrix} p \\ u \end{pmatrix} \quad (3.40)$$

such as seen in Figure 3.12.

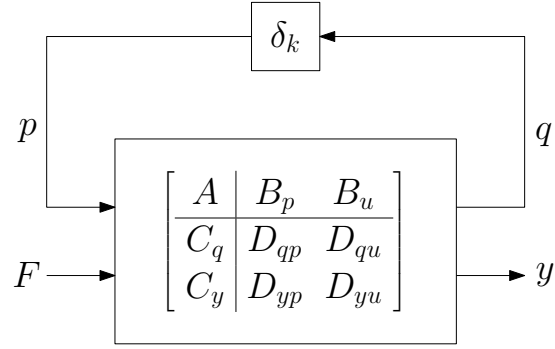


Figure 3.12. Uncertainty representation of a spring mass damper system.

We can also represent uncertainties in G_{unc} as a Δ block. We use LFT toolbox to create a Δ block such as in following figure.

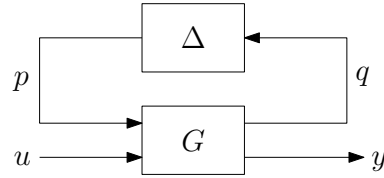


Figure 3.13. Uncertainty representation of G .

where $\Delta = \text{diag}(\delta_1 I_{n_1}, \delta_2 I_{n_2}, \dots, \delta_k I_{n_k})$ such that $\|\delta_i\| \leq 1 \quad \forall i = 1 : k$ and

$$\begin{pmatrix} q \\ y \end{pmatrix} = \underbrace{\begin{bmatrix} A & B_p & B_u \\ C_q & D_{qp} & D_{qu} \\ C_y & D_{yp} & D_{yu} \end{bmatrix}}_G \begin{pmatrix} p \\ u \end{pmatrix}. \quad (3.41)$$

We have 2 uncertain parameters c_F and v since we define $c_R = c_F$ such that

$$\Delta = \begin{bmatrix} \delta_{c_F} I_2 & 0 \\ 0 & \delta_v I_7 \end{bmatrix}. \quad (3.42)$$

If we represent G_{unc} as the interconnection seen in Figure 3.13, our control problem became

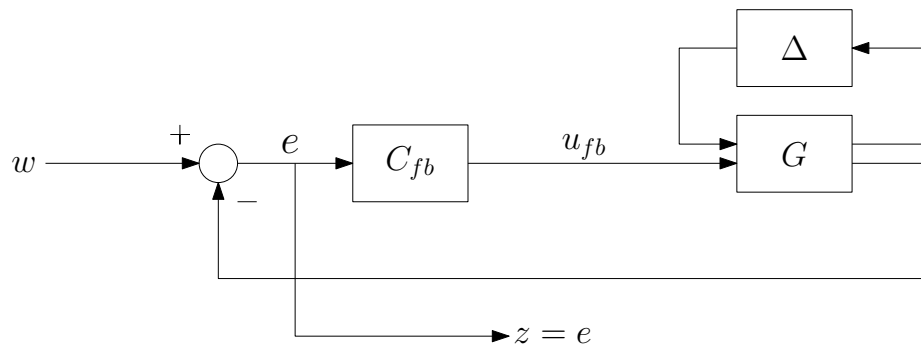


Figure 3.14. Closed loop system with uncertainty block.

3.6. Robust Feedforward Control Synthesis

Since the joint search for a controller C and multipliers is non-convex in general, we use D-K iteration method for most system. But some problems allow for jointly convex search for C and multipliers such as robust estimation and robust feedforward control. Because unlike the general case, the Δ -block and C_{ff} do not interact in the feedback loop which leads to a convex solution [19].

Feedforward controller is feasible for reference tracking problems where the reference signal is treated as a disturbance which is same with our problem.

Our feedback controller C_{fb} is fixed and closed loop system is stable. We add a feedforward controller to this stable system to improve transient response. We design this feedforward controller for the closed loop feedback system \tilde{G} as in Figure 3.15.

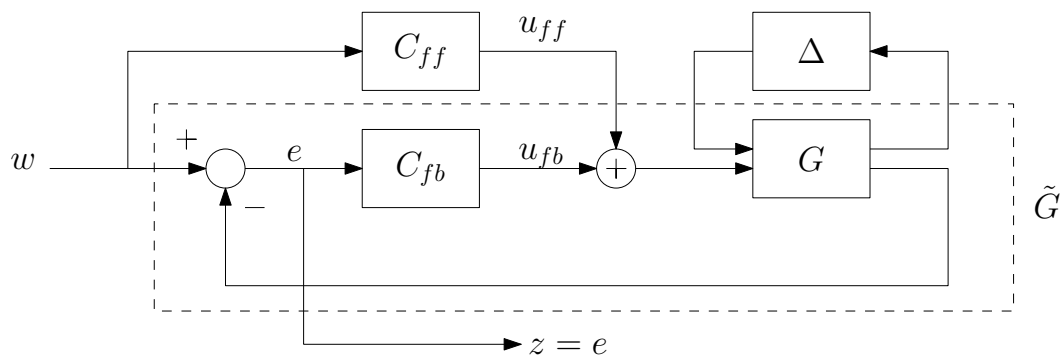


Figure 3.15. Feedforward and feedback controllers.

We can combine feedback controller and G into \tilde{G} as seen in Figure 3.16

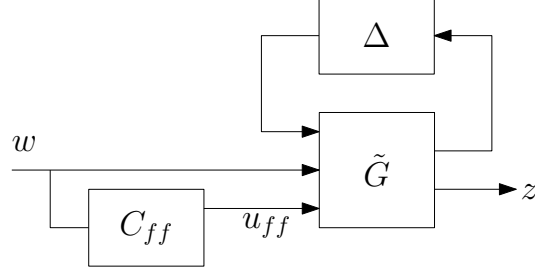


Figure 3.16. Feedforward controller for \tilde{G} .

where

$$\begin{pmatrix} q \\ z \end{pmatrix} = \underbrace{\begin{bmatrix} A & B_p & B_w & B_u \\ C_q & D_{qp} & D_{qw} & D_{qu} \\ C_z & D_{zp} & D_{zw} & D_{zu} \end{bmatrix}}_{\tilde{G}} \begin{pmatrix} p \\ w \\ u \end{pmatrix} \quad (3.43)$$

and

$$u = \underbrace{\begin{bmatrix} A_C & B_C \\ C_C & D_C \end{bmatrix}}_{C_{ff}} w. \quad (3.44)$$

If we combine \tilde{G} and C_{ff} we obtain an interconnection between closed loop system G_{cl} and Δ as seen in Figure 3.17 where

$$\begin{pmatrix} q \\ z \end{pmatrix} = \underbrace{\begin{bmatrix} A & B_u C_C & B_p & B_w + B_u D_C \\ 0 & A_C & 0 & B_C \\ C_q & D_{qu} C_C & D_{qp} & D_{qw} + D_{qu} D_C \\ C_z & D_{zu} C_C & D_{zp} & D_{zw} + D_{zu} D_C \end{bmatrix}}_{G_{cl}} \begin{pmatrix} p \\ w \end{pmatrix}. \quad (3.45)$$

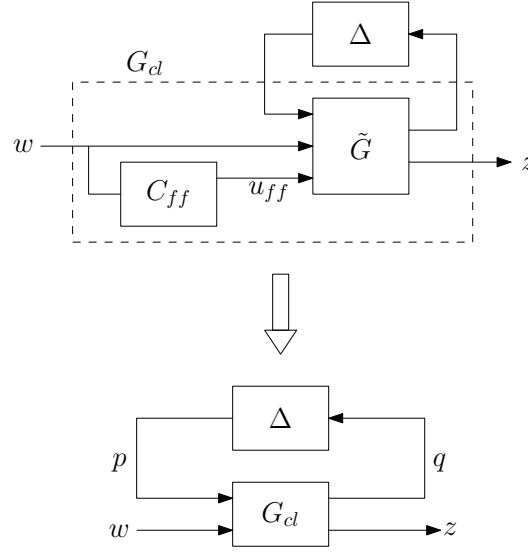
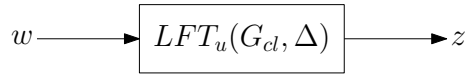


Figure 3.17. System in LFT form.

3.6.1. Performance Objective

It may not be possible to measure disturbance signal in real disturbance attenuation problem. But in our case, reference signal is considered as disturbance and output is error between output of the vehicle model and this reference.

Figure 3.18. G_{cl} and Δ in LFT form.

The objective is to design C_{ff} such that $LFT_u(G_{cl}, \Delta)$ is robustly stable and the closed loop system \mathcal{L}_2 -gain is bounded by some scalar $\gamma > 0$.

Up to this point, we derive single track model using small angle assumption and we design a feedback controller which is working great for nominal vehicle model. But it is seen that feedback cannot respond well for uncertainties in this nominal vehicle model. We propose use of feedforward controller to deal with this uncertainties. Before we explain synthesis of feedforward controller, we give some basic information about convex optimization, linear matrix inequalities and integral quadratic constraints in the following two chapter.

4. CONVEX OPTIMIZATION AND LINEAR MATRIX INEQUALITIES

4.1. Convex Optimization

First of all, definitions of convex sets and convex functions are given.

Definition 4.1. (Convex Sets) *Let \mathcal{X} be linear vector space. A set $\mathcal{S} \subseteq \mathcal{X}$ is convex if*

$$x, y \in \mathcal{S} \Rightarrow \lambda x + (1 - \lambda)y \in \mathcal{S}, \quad \forall \lambda \in (0, 1). \quad (4.1)$$

Definition 4.2. (Convex Function [20]) *Let \mathcal{S} be a convex set. A function $f : \mathcal{S} \rightarrow \mathbb{R}$ is convex if*

$$x, y \in \mathcal{S} \Rightarrow f(\lambda x + (1 - \lambda)y) \leq \lambda f(x) + (1 - \lambda)f(y), \quad \forall \lambda \in (0, 1) \quad (4.2)$$

holds.

The problem of minimizing convex functions is convex optimization. The form of a convex optimization problem is

$$\begin{aligned} \text{minimize} & \quad : f(x) \\ \text{subject to} & \quad : x \in \mathcal{S} \end{aligned} \quad (4.3)$$

where the function $f : \mathcal{S} \rightarrow \mathbb{R}$ is convex and \mathcal{S} is a convex set.

4.1.1. Local and Global Minima

Finding global minima is the goal of optimization. But local minima pose a

problem for finding global minima. We are trying to find x^* such as

$$f(x^*) \leq f(x), \quad \forall x \in \mathcal{S} \quad (4.4)$$

Proposition 4.3. (Global minima [21]) *Suppose that $f : \mathcal{S} \rightarrow \mathbb{R}$ is convex. Every local optimal solution of f is a global optimal solution. Moreover, if f is strictly convex, then the global optimal solution is unique.*

A proof of the above proposition can be found in [21].

4.2. Linear Matrix Inequalities

First of all we need to define definiteness to understand linear matrix inequalities. Let Q be a real square symmetric matrix, $Q \in \mathbb{R}^{n \times n}$ and $\forall x \in \mathbb{R}^n$. Q is ‘positive definite’ if

$$x^T Q x > 0, \quad \forall x \neq 0 \quad (4.5)$$

and Q is ‘positive semi-definite’ if

$$x^T Q x \geq 0, \quad \forall x \quad (4.6)$$

If Q is a complex matrix where $Q = Q^* \in \mathbb{C}^{n \times n}$ and $\forall x \in \mathbb{C}^n$, it is positive definite if 4.5 holds and then Q will be Hermitian [22].

Definition 4.4. (LMI [23]) *A linear matrix inequality (LMI) is a constraint of the form*

$$F(x) := F_0 + x_1 F_1 + \dots + x_n F_n \prec 0 \quad (4.7)$$

where $x \in \mathbb{R}^m$ is the variable and F_i ’s are real symmetric matrices

Proposition 4.5. (Set of LMIs [21]) *A set of LMIs such as*

$$F_1(x) \prec 0, F_2(x) \prec 0, \dots, F_k(x) \prec 0 \quad (4.8)$$

hold if and only if

$$F(x) := \begin{pmatrix} F_1(x) & 0 & \dots & 0 \\ 0 & F_2(x) & \dots & 0 \\ \vdots & \vdots & \ddots & \vdots \\ 0 & 0 & \dots & F_k(x) \end{pmatrix} \prec 0. \quad (4.9)$$

Example: Consider an autonomous linear system

$$\dot{x} = Ax \quad (4.10)$$

where $A : \mathbb{R}^n \rightarrow \mathbb{R}^n$. Let $V(x)$ be Lyapunov function

$$V(x) = x^T P x \succ 0 \quad (4.11)$$

derivative of $V(x)$ will be

$$\dot{V}(x) = x^T A^T P x + x^T P A x \prec 0 \quad (4.12)$$

Then, system is stable if and only if there exist a matrix $P \succ 0$ such that

$$A^T P + P A \prec 0. \quad (4.13)$$

This two inequalities can be combined into

$$\begin{pmatrix} A^T P + P A & 0 \\ 0 & -P \end{pmatrix} \prec 0. \quad (4.14)$$

Proposition 4.6. (Schur Complement [22]) *Following statements are equivalent:*

(i)

$$\begin{aligned} \Phi_{22} &\prec 0 \\ \Phi_{11} - \Phi_{12}\Phi_{22}^{-1}\Phi_{12}^T &\prec 0 \end{aligned} \quad (4.15)$$

(ii)

$$\Phi = \begin{pmatrix} \Phi_{11} & \Phi_{12} \\ \Phi_{12}^T & \Phi_{22} \end{pmatrix} \prec 0 \quad (4.16)$$

A set of non-linear inequalities (4.15) can be converted to equivalent linear matrix inequality (4.16) by ‘Schur Complement’ which is used to create suitable LMIs for solver in Chapter 6.

We design a controller where the closed loop system \mathcal{L}_2 -gain is bounded by some scalar $\gamma > 0$. We encountered a problem caused by γ^{-1} such that

$$\begin{aligned} \gamma &\succ 0 \\ \phi_{11} - \phi_{12}\gamma^{-1}\phi_{12}^T &\succ 0 \end{aligned} \quad (4.17)$$

We deal with non-linear γ^{-1} applying ‘Schur Complement’. Then equivalent LMI which we need to solve will be

$$\phi = \begin{pmatrix} \phi_{11} & \phi_{12} \\ \phi_{12}^T & \gamma I \end{pmatrix} \succ 0. \quad (4.18)$$

5. SYSTEM ANALYSIS VIA IQCs

In this chapter, integral quadratic constraint (IQC) is described. IQC is used to analyze stability of interconnection shown in Figure 5.2. G is stable LTI system and Δ represent uncertainties. A theorem described in [9] is given to analyze stability of this interconnection. This theorem gives a frequency dependent inequality for stability analysis of G - Δ interconnection. Using KYP lemma, this frequency dependent inequality can be solved by replacing frequency dependence with a new decision matrix [24]. Then we can able to solve resulting inequality numerically. Dual IQCs is explained. We use dual IQC for our problem in this study because of the nature of feedforward problem.

5.1. Stability Analysis

Let G and Δ be stable. We inject two input into the interconnection (5.2) to see if the interconnection of G and Δ is stable or not such as

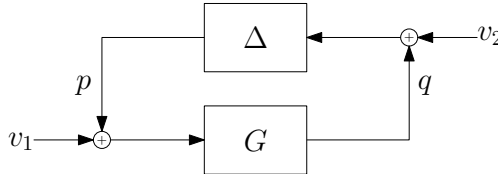


Figure 5.1. Disturbed interconnection of G and Δ .

where

$$\begin{aligned}\tilde{p} &= v_1 + \Delta q \\ q &= v_2 + G\tilde{p}\end{aligned}$$

which can be written as

$$\begin{pmatrix} I & -\Delta \\ -G & I \end{pmatrix} \begin{pmatrix} \tilde{p} \\ q \end{pmatrix} = \begin{pmatrix} v_1 \\ v_2 \end{pmatrix} \quad (5.1)$$

If we solve above equation for $\begin{pmatrix} \tilde{p} \\ q \end{pmatrix}$,

$$\begin{pmatrix} \tilde{p} \\ q \end{pmatrix} = \begin{pmatrix} I & -\Delta \\ -G & I \end{pmatrix}^{-1} \begin{pmatrix} v_1 \\ v_2 \end{pmatrix} \quad (5.2)$$

$$= \begin{pmatrix} I + \Delta(I - G\Delta)^{-1}G & \Delta(I - G\Delta)^{-1} \\ (I - G\Delta)^{-1}G & (I - G\Delta)^{-1} \end{pmatrix}^{-1} \begin{pmatrix} v_1 \\ v_2 \end{pmatrix} \quad (5.3)$$

Assume that $(I - G\Delta)^{-1}$ exists for $\forall \Delta \in \mathbb{B}_\Delta$, then interconnection G and Δ is well-posed. If $(I - G\Delta)^{-1}$ is stable, the system (5.1) is robustly stable. Robust stability can also be analyzed using IQCs.

5.2. Integral Quadratic Constraints

First we need to give definition of IQC since we use it to analyze stability of interconnection between G and Δ via IQCs.

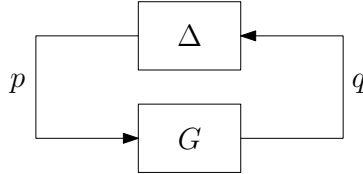


Figure 5.2. Interconnection of G and Δ .

Definition 5.1. (Integral Quadratic Constraint) *Let $\Pi = \Pi^* \in \mathcal{L}_\infty$. Then Δ is said to satisfy the IQC associated with Π if*

$$\left\langle \begin{pmatrix} v \\ \Delta v \end{pmatrix}, \Pi \begin{pmatrix} v \\ \Delta v \end{pmatrix} \right\rangle \geq 0 \quad \forall v \in \mathcal{L}_2. \quad (5.4)$$

Following theorem defines criteria for the stability of the $G - \Delta$ interconnection.

Theorem 5.2. [9] *Let G be stable and suppose there exists a $\Pi = \Pi^* \in \mathcal{L}_\infty$ such that*

- i) $\forall \tau \in [0, 1]$, the interconnection of G and $\tau\Delta$ is well-posed;
ii) $\forall \tau \in [0, 1]$, the IQC defined by Π is satisfied by $\tau\Delta$ such that

$$\left\langle \begin{pmatrix} q \\ \tau\Delta q \end{pmatrix}, \Pi \begin{pmatrix} q \\ \tau\Delta q \end{pmatrix} \right\rangle \geq 0 \quad \forall q \in \mathcal{L}_2 \quad (5.5)$$

iii) G satisfies

$$\begin{pmatrix} G(j\omega) \\ I \end{pmatrix}^* \Pi(j\omega) \begin{pmatrix} G(j\omega) \\ I \end{pmatrix} \prec 0, \quad \forall \omega \in \mathbb{R} \cup \{\infty\}. \quad (5.6)$$

Then, the feedback interconnection of G and Δ is stable.

Remark. Consider the system shown in Figure 5.3. If robust quadratic performance specification from w to z such that

$$\int_0^\infty \begin{pmatrix} w(t) \\ z(t) \end{pmatrix}^T \begin{pmatrix} -\gamma I & 0 \\ 0 & \gamma^{-1} I \end{pmatrix} \begin{pmatrix} w(t) \\ z(t) \end{pmatrix} dt \leq 0 \quad (5.7)$$

holds, then controller synthesis based on solving this specification guarantees that the \mathcal{L}_2 -gain from w to z is robustly smaller than γ [25].

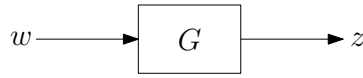


Figure 5.3. Performance of a system G .

We can simply show that the H_∞ -norm of a system is smaller than γ such that

$$\begin{aligned} \|G\|_\infty < \gamma &\Leftrightarrow \sup_{\omega \in \mathbb{R}} \bar{\sigma}(G(j\omega)) < \gamma \\ &\Leftrightarrow \lambda_{\max}(G(j\omega)^* G(j\omega)) < \gamma^2 \quad \forall \omega \in \mathbb{R} \cup \{\infty\} \\ &\Leftrightarrow G(j\omega)^* G(j\omega) \prec \gamma^2 I \quad \forall \omega \in \mathbb{R} \cup \{\infty\} \\ &\Leftrightarrow \frac{1}{\gamma} G(j\omega)^* G(j\omega) \prec \gamma I \quad \forall \omega \in \mathbb{R} \cup \{\infty\} \end{aligned}$$

$$\Leftrightarrow \begin{pmatrix} G(j\omega) \\ I \end{pmatrix}^T \begin{pmatrix} \gamma^{-1}I & 0 \\ 0 & -\gamma I \end{pmatrix} \begin{pmatrix} G(j\omega) \\ I \end{pmatrix} \prec 0 \quad \forall \omega \in \mathbb{R} \cup \{\infty\}$$

which is in the form of (5.6).

5.3. Robust Performance Problem

We focus on robust stability and performance of the system (3.45) as seen in Figure 3.17 in this study. If G_{cl} is stable, the G_{cl} and $\tau\Delta$ interconnection is well-posed and

$$\begin{pmatrix} G_{cl}(j\omega) \\ I \end{pmatrix}^* \begin{pmatrix} \Pi_{11}(j\omega) & 0 & \Pi_{12}(j\omega) & 0 \\ 0 & \gamma I & 0 & 0 \\ \Pi_{11}(j\omega)^* & 0 & \Pi_{22}(j\omega) & 0 \\ 0 & 0 & 0 & -\gamma^{-1}I \end{pmatrix} \begin{pmatrix} G_{cl}(j\omega) \\ I \end{pmatrix} \prec 0 \quad (5.8)$$

where

$$\Pi = \begin{pmatrix} \Pi_{11} & \Pi_{12} \\ \Pi_{12}^* & \Pi_{22} \end{pmatrix} \quad (5.9)$$

satisfies (5.5), then the system (3.45) is robustly stable and the \mathcal{L}_2 -gain from w to z is smaller than γ [11].

5.3.1. Dual IQCs

Dual IQCs are used for analysis in this study because of the nature of feedforward control problem. We now give following lemma to create equivalent dual form of inequality (5.6).

Lemma 5.3. [26] *Let $\mathcal{G} \in \mathbb{C}^{(m+n) \times m}$ have full column-rank and $M = M^* \in \mathbb{C}^{(m+n) \times (m+n)}$ be such that $\text{in}(M) = (m, n, 0)$. Then, $\mathcal{G}^* \Pi \mathcal{G} \succ 0$ if and only if $\mathcal{G}_\perp^* \Pi^{-1} \mathcal{G}_\perp \prec 0$, where \mathcal{G}_\perp forms a basis for the orthogonal complement of the image of \mathcal{G} .*

If inequality (5.6) holds, we can assume that $\Pi_{11} \succ 0$ and Π has as many negative eigenvalues as the number of inputs of G , and since

$$\mathbf{in}(\Pi) = \mathbf{in}(\Pi_{11}) + \mathbf{in}(\Pi_{22} - \Pi_{12}^* \Pi_{11}^{-1} \Pi_{12}), \quad (5.10)$$

we obtain

$$\Pi_{11} \succ 0 \quad \text{and} \quad \Pi_{22} - \Pi_{12}^* \Pi_{11}^{-1} \Pi_{12} \prec 0 \quad (5.11)$$

as discussed in [11]. If we apply Lemma 5.3 to Inequality (5.6) for the G - Δ interconnection, we obtain

$$\begin{pmatrix} I \\ -G(j\omega)^* \end{pmatrix}^* \Pi(j\omega)^{-1} \begin{pmatrix} I \\ -G(j\omega)^* \end{pmatrix} \succ 0, \quad \forall \omega \in \mathbb{R} \cup \{\infty\}. \quad (5.12)$$

We can define

$$\Pi^{-1} =: \Theta = \begin{pmatrix} \Theta_{11} & \Theta_{12} \\ \Theta_{12}^* & \Theta_{22} \end{pmatrix} \quad (5.13)$$

as discussed in [11] where

$$\Theta_{22} = \Theta_{22}^* \prec 0 \quad \text{and} \quad \Theta_{11} - \Theta_{12} \Theta_{22}^{-1} \Theta_{12}^* \succ 0. \quad (5.14)$$

Θ can be factorized as

$$\Theta = \phi N \phi^* \quad (5.15)$$

and it can be partitioned as

$$\phi N \phi^* = \begin{pmatrix} -\phi_1 \\ -\phi_2 \end{pmatrix} N \begin{pmatrix} -\phi_1^* & -\phi_2^* \end{pmatrix} = \begin{pmatrix} \phi_1 N \phi_1^* & \phi_1 N \phi_2^* \\ \phi_2 N \phi_1^* & \phi_2 N \phi_2^* \end{pmatrix} \quad (5.16)$$

where, by the structure of Θ ,

$$\Theta_{22} = \phi_2 N \phi_2^* \prec 0. \quad (5.17)$$

We can equivalently write (5.17) as

$$\left[\begin{array}{c|c} -A_{\phi_2}^T & -C_{\phi_2}^T \\ \hline -B_{\phi_2}^T & -D_{\phi_2}^T \end{array} \right]^* N \left[\begin{array}{c|c} -A_{\phi_2}^T & -C_{\phi_2}^T \\ \hline -B_{\phi_2}^T & -D_{\phi_2}^T \end{array} \right] \prec 0. \quad (5.18)$$

Inequality (5.12) can also be written as

$$(\star)^* \begin{pmatrix} -\phi_1 \\ -\phi_2 \end{pmatrix} N \begin{pmatrix} -\phi_1^* & -\phi_2^* \end{pmatrix} \begin{pmatrix} I \\ -G(j\omega)^* \end{pmatrix} \succ 0, \quad \forall \omega \in \mathbb{R} \cup \{\infty\} \quad (5.19)$$

where

$$G = \left[\begin{array}{c|c} A & B \\ \hline C & D \end{array} \right], \quad \begin{pmatrix} -\phi_1^* & -\phi_2^* \end{pmatrix} = \left[\begin{array}{cc|cc} -A_{11}^T & 0 & -C_{11}^T & 0 \\ -A_{12}^T & -A_{22}^T & -C_{12}^T & -C_{22}^T \\ \hline -B_1^T & -B_2^T & -D_1^T & -D_2^T \end{array} \right] \quad (5.20)$$

and

$$\begin{aligned} \begin{pmatrix} -\phi_1^* & -\phi_2^* \end{pmatrix} \begin{pmatrix} I \\ -G^* \end{pmatrix} &= \left[\begin{array}{ccc|c} -A_{11}^T & 0 & 0 & -C_{11}^T \\ -A_{12}^T & -A_{22}^T & -C_{12}^T B^T & -C_{12}^T + C_{22}^T D^T \\ 0 & 0 & -A^T & -C^T \\ \hline -B_1^T & -B_2^T & D_2^T B^T & -D_1^T + D_2^T D^T \end{array} \right] \\ &=: \left[\begin{array}{c|c} -\mathcal{A}^T & -\mathcal{C}^T \\ \hline -\mathcal{B}^T & -\mathcal{D}^T \end{array} \right]. \end{aligned} \quad (5.21)$$

If 5.21 is stable and conditions (5.18) and (5.19) holds, then the G - Δ interconnection is robustly stable.

5.3.2. Dual IQCs in State-space

We need to convert conditions (5.18) and (5.19) into feasible LMIs since we cannot solve them for all frequencies. We use KYP lemma for this purpose. KYP lemma is basis of relation between frequency dependent matrix inequalities and feasible LMIs.

Lemma 5.4. (KYP [24]) *Given*

$$\mathcal{G} = \left[\begin{array}{c|c} \mathcal{A} & \mathcal{B} \\ \hline \mathcal{C} & \mathcal{D} \end{array} \right] \quad (5.22)$$

and $M = M^T$, the condition

$$G(j\omega)^* M G(j\omega) \prec 0, \quad \forall \omega \in \mathbb{R} \quad (5.23)$$

holds if and only if, $\exists X = X^T$ such that

$$\begin{pmatrix} I & 0 \\ \mathcal{A} & \mathcal{B} \\ \mathcal{C} & \mathcal{D} \end{pmatrix}^* \begin{pmatrix} 0 & X & 0 \\ X & 0 & 0 \\ 0 & 0 & M \end{pmatrix} \begin{pmatrix} I & 0 \\ \mathcal{A} & \mathcal{B} \\ \mathcal{C} & \mathcal{D} \end{pmatrix} \prec 0 \quad (5.24)$$

Moreover, if $\mathcal{C}^T M \mathcal{C} \succeq 0$ then, \mathcal{A} is Hurwitz if and only if $X = X^T \succ 0$.

The proof can be found in [24].

Now frequency dependent matrix inequality (5.18) can be transformed into a feasible LMI by KYP lemma. (5.18) holds if $\exists X = X^T$ such that

$$\begin{pmatrix} -A_{\phi_2}^T & -C_{\phi_2}^T \\ I & 0 \\ -B_{\phi_2}^T & -D_{\phi_2}^T \end{pmatrix}^* \begin{pmatrix} 0 & X & 0 \\ X & 0 & 0 \\ 0 & 0 & N \end{pmatrix} \begin{pmatrix} -A_{\phi_2}^T & -C_{\phi_2}^T \\ I & 0 \\ -B_{\phi_2}^T & -D_{\phi_2}^T \end{pmatrix} \prec 0. \quad (5.25)$$

Inequality (5.19) holds if $\exists Y = Y^T \succ 0$ such that

$$\begin{pmatrix} -\mathcal{A}^T & -\mathcal{C}^T \\ -\mathcal{B}^T & -\mathcal{D}^T \\ I & 0 \end{pmatrix}^* \begin{pmatrix} 0 & Y & 0 \\ Y & 0 & 0 \\ 0 & 0 & N \end{pmatrix} \begin{pmatrix} -\mathcal{A}^T & -\mathcal{C}^T \\ -\mathcal{B}^T & -\mathcal{D}^T \\ I & 0 \end{pmatrix} \prec 0. \quad (5.26)$$

In order to guarantee (5.21) to be stable we give the following condition.

Theorem 5.5. ([11]) *Matrix A is Hurwitz and the conditions (5.18) and (5.19) hold if and only if there exist solutions $Y = Y^T$ and $X = X^T$ of LMIs (5.25) and (5.26) that are coupled as*

$$\mathcal{Y} = \begin{pmatrix} Y_{22} - X & Y_{23} & Y_{24} \\ Y_{23}^T & Y_{33} & Y_{34} \\ Y_{24}^T & Y_{34}^T & (Y - \hat{X})^{-1} \end{pmatrix} \succ 0. \quad (5.27)$$

Condition (5.27) can be partitioned as

$$\begin{pmatrix} T^T Y T - \begin{pmatrix} X & 0 \\ 0 & 0 \end{pmatrix} & T^T \\ T & (Y - \hat{X})^{-1} \end{pmatrix} \succ 0 \quad (5.28)$$

as discussed in [11] where $T = \begin{pmatrix} 0 & 0 \\ I & 0 \\ 0 & I \end{pmatrix}$. With respect to the ‘Schur Complement Formula’, this is equivalent to

$$T^T Y T - \begin{pmatrix} X & 0 \\ 0 & 0 \end{pmatrix} - T^T (Y - \hat{X}) T \succ 0 \text{ and } (Y - \hat{X})^{-1} \succ 0 \quad (5.29)$$

which can be written equivalently

$$T^T \hat{X} T - \begin{pmatrix} X & 0 \\ 0 & 0 \end{pmatrix} \succ 0. \quad (5.30)$$

Also dual of inequality (5.8) is used with dynamic multipliers for closed loop system (3.45) such as

$$\begin{pmatrix} I \\ -G_{cl}^* \end{pmatrix}^* \begin{pmatrix} \phi_1 N \phi_1^* & 0 & \phi_1 N \phi_2^* & 0 \\ 0 & \gamma I & 0 & 0 \\ \phi_2 N \phi_1^* & 0 & \phi_2 N \phi_2^* & 0 \\ 0 & 0 & 0 & -\gamma^{-1} \end{pmatrix} \begin{pmatrix} I \\ -G_{cl}^* \end{pmatrix} \succ 0, \quad (5.31)$$

then the system (3.45) is robustly stable and \mathcal{L}_2 -gain of performance channel is smaller than γ . We can write this inequality by separating the static part and dynamic part such as

$$\underbrace{(*)^* (*)^* \begin{pmatrix} N & 0 & 0 \\ 0 & \gamma I & 0 \\ 0 & 0 & -\gamma^{-1} \end{pmatrix}}_M \underbrace{\begin{pmatrix} -\phi_1^* & 0 & -\phi_2^* & 0 \\ 0 & I & 0 & 0 \\ 0 & 0 & 0 & I \end{pmatrix}}_{\mathcal{G}} \begin{pmatrix} I \\ -G_{cl}^* \end{pmatrix} \succ 0. \quad (5.32)$$

Inequality (5.32) can be written as

$$\mathcal{G}^* M \mathcal{G} \succ 0. \quad (5.33)$$

We can define

$$\mathcal{G} := \begin{pmatrix} -\phi_1^* & 0 & -\phi_2^* & 0 \\ 0 & I & 0 & 0 \\ 0 & 0 & 0 & I \end{pmatrix} \begin{pmatrix} I \\ -G_{cl}^* \end{pmatrix} \quad (5.34)$$

$$= \left[\begin{array}{cc|c} -\mathcal{A}^T & 0 & -\mathcal{C}^T \\ -C_C^T \mathcal{B}_u^T & -A_C^T & -C_C^T \mathcal{D}_u^T \\ \hline -\mathcal{B}_\phi^T & 0 & -\mathcal{D}_\phi^T \\ 0 & 0 & -\mathcal{D}_p^T \\ -\mathcal{B}_w^T - D_C^T \mathcal{B}_u^T & -B_C^T & -\mathcal{D}_w^T - D_C^T \mathcal{D}_{qu}^T \end{array} \right] \quad (5.35)$$

where

$$\begin{pmatrix} -\phi_1^* & 0 & -\phi_2^* & 0 \\ 0 & I & 0 & 0 \\ 0 & 0 & 0 & I \end{pmatrix} \begin{pmatrix} I \\ -\tilde{G}^* \end{pmatrix} := \left[\begin{array}{c|c} -\mathcal{A}^T & -\mathcal{C}^T \\ \hline -\mathcal{B}_\phi^T & -\mathcal{D}_\phi^T \\ 0 & -\mathcal{D}_p^T \\ -\mathcal{B}_w^T & -\mathcal{D}_w^T \\ -\mathcal{B}_u^T & -\mathcal{D}_u^T \end{array} \right]$$

$$:= \left[\begin{array}{ccc|cc} -A_{11}^T & 0 & 0 & -C_{11}^T & 0 \\ -A_{12}^T & -A_{22}^T & -C_{12}^T B_p^T & -C_{12}^T + C_{22}^T D_{qp}^T & C_{22}^T D_{zp}^T \\ 0 & 0 & -A^T & -C_q^T & -C_z^T \\ \hline -B_1^T & -B_2^T & D_2^T B_p^T & -D_1^T + D_2^T D_{qp}^T & D_2^T D_{zp}^T \\ 0 & 0 & 0 & 0 & I \\ 0 & 0 & -B_w^T & -D_{qw}^T & -D_{zw}^T \\ 0 & 0 & -B_u^T & -D_{qu}^T & -D_{zu}^T \end{array} \right] \quad (5.36)$$

But we need to convert (5.33) into a feasible LMI form since we cannot solve it for all frequencies. KYP lemma is used to convert frequency dependent matrix inequalities to feasible LMIs. Applying KYP lemma to (5.33) we obtain the following inequality.

If $\exists \mathcal{Y} = \mathcal{Y}^T$ such that

$$(\star)^T \begin{pmatrix} 0 & \mathcal{Y} & 0 \\ \mathcal{Y} & 0 & 0 \\ 0 & 0 & M \end{pmatrix} \underbrace{\begin{pmatrix} -\mathcal{A}^T & 0 & -\mathcal{C}^T \\ -C_C^T \mathcal{B}_u^T & -A_C^T & -C_C^T \mathcal{D}_u^T \\ I & 0 & 0 \\ 0 & I & 0 \\ -\mathcal{B}_\phi^T & 0 & -\mathcal{D}_\phi^T \\ 0 & 0 & -\mathcal{D}_p^T \\ -\mathcal{B}_w^T - D_C^T \mathcal{B}_u^T & -B_C^T & -\mathcal{D}_w^T - D_C^T \mathcal{D}_{qu}^T \end{pmatrix}}_{\begin{pmatrix} A & B \\ I & 0 \\ C & D \end{pmatrix}} \succ 0, \quad (5.37)$$

then stability is guaranteed and \mathcal{L}_2 -gain of performance channel is robustly smaller than γ .

Following theorem give sufficient condition for the system (3.45) to be robustly stable and its \mathcal{L}_2 -gain to be less than γ .

Theorem 5.6. ([11]) *There exists a stable feedforward controller that satisfies (5.32) if and only if there exist an $X = X^T$ that satisfies (5.25) and $Y = Y^T$, $\hat{X} = \hat{X}^T$, \mathbf{A}_C , \mathbf{B}_C , \mathbf{C}_C and \mathbf{D}_C such that*

$$(\star)^T \begin{pmatrix} 0 & I & 0 \\ I & 0 & 0 \\ 0 & 0 & M \end{pmatrix}$$

$$\times \begin{pmatrix} -\hat{X}\mathcal{A}^T & -\hat{X}\mathcal{A}^T & -\hat{X}\mathcal{C}^T \\ \mathbf{A}_C^T & -Y\mathcal{A}^T - \mathbf{C}_C^T\mathcal{B}_u^T & -Y\mathcal{C}^T - \mathbf{C}_C^T\mathcal{D}_u^T \\ \hline I & 0 & 0 \\ 0 & I & 0 \\ \hline -\mathcal{B}_\phi^T & -\mathcal{B}_\phi^T & -\mathcal{D}_\phi^T \\ 0 & 0 & -\mathcal{D}_p^T \\ -\mathcal{B}_w^T - \mathbf{D}_C^T\mathcal{B}_u^T - \mathbf{B}_C^T & -\mathcal{B}_w^T - \mathbf{D}_C^T\mathcal{B}_u^T & -\mathcal{D}_w^T - \mathbf{D}_C^T\mathcal{D}_u^T \end{pmatrix} \succ 0, \quad (5.38)$$

$$T^T\hat{X}T - \begin{pmatrix} X & 0 \\ 0 & 0 \end{pmatrix} \succ 0 \quad (5.39)$$

and

$$Y - \hat{X} \succ 0 \quad (5.40)$$

are satisfied. When these LMIs are feasible, then the controller can be obtained from

$$A_C^T = (-\mathbf{A}_C^T - Y\mathcal{A}^T + C_C^T\mathcal{B}_u^T)(\hat{X} - Y)^{-1} \quad (5.41)$$

$$B_C^T = (\mathbf{B}_C^T)(\hat{X} - Y)^{-1} \quad (5.42)$$

$$C_C^T = \mathbf{C}_C^T \quad (5.43)$$

$$D_C^T = \mathbf{D}_C^T \quad (5.44)$$

Proof. We apply congruence transformation to transform Inequality (5.37) into suitable LMI form by removing bilinear terms. As discussed in [26], we can assume that \mathcal{Y} can

be partitioned as

$$\mathcal{Y} = \left(\begin{array}{ccc|c} \mathcal{Y}_{11} & \mathcal{Y}_{12} & \mathcal{Y}_{13} & \mathcal{Y}_{14} \\ \star & \mathcal{Y}_{22} & \mathcal{Y}_{23} & \mathcal{Y}_{24} \\ \star & \star & \mathcal{Y}_{33} & \mathcal{Y}_{34} \\ \hline \star & \star & \star & \mathcal{Y}_{44} \end{array} \right) = \left(\begin{array}{c|c} Y & I \\ \hline I & (Y - \hat{X})^{-1} \end{array} \right) \quad (5.45)$$

Then, we can apply following congruence transformation where $W = \begin{pmatrix} I & I \\ \hat{X} - Y & 0 \end{pmatrix}$

$$(\star)^T (\star)^T \left(\begin{array}{ccc|c} 0 & \mathcal{Y} & 0 & \\ \mathcal{Y} & 0 & 0 & \\ \hline 0 & 0 & M & \end{array} \right) \underbrace{\left(\begin{array}{cc} A & B \\ \hline I & 0 \\ \hline C & D \end{array} \right)}_a \underbrace{\left(\begin{array}{c|c} W & 0 \\ \hline 0 & I \end{array} \right)}_b \succ 0, \quad (5.46)$$

If we multiply a and b we obtain

$$(\star)^T \left(\begin{array}{ccc|c} 0 & \mathcal{Y} & 0 & \\ \mathcal{Y} & 0 & 0 & \\ \hline 0 & 0 & M & \end{array} \right) \left(\begin{array}{cc} AW & B \\ \hline W & 0 \\ \hline CW & D \end{array} \right) \succ 0, \quad (5.47)$$

Above inequality still holds, if we multiply this with identity $(e \times f)$ such as;

$$\underbrace{(\star)^T (\star)^T (\star)^T}_{c} \underbrace{\left(\begin{array}{ccc|c} 0 & \mathcal{Y} & 0 & \\ \mathcal{Y} & 0 & 0 & \\ \hline 0 & 0 & M & \end{array} \right)}_d \underbrace{\left(\begin{array}{ccc} W & 0 & 0 \\ 0 & W & 0 \\ 0 & 0 & I \end{array} \right)}_e \underbrace{\left(\begin{array}{ccc} W^{-1} & 0 & 0 \\ 0 & W^{-1} & 0 \\ 0 & 0 & I \end{array} \right)}_f \underbrace{\left(\begin{array}{cc} AW & B \\ \hline W & 0 \\ \hline CW & D \end{array} \right)}_g \succ 0, \quad (5.48)$$

If we multiply d from left and right with c and e respectively, and multiply f and g we

obtain:

$$(\star)^T \left(\begin{array}{cc|c} 0 & W^T \mathcal{Y} W & 0 \\ W^T \mathcal{Y} W & 0 & 0 \\ \hline 0 & 0 & M \end{array} \right) \left(\begin{array}{cc} W^{-1} A W & W^{-1} B \\ \hline I & 0 \\ C W & D \end{array} \right) \succ 0, \quad (5.49)$$

which can be transform into

$$(\star)^T \left(\begin{array}{cc|c} 0 & I & 0 \\ I & 0 & 0 \\ \hline 0 & 0 & M \end{array} \right) \left(\begin{array}{cc} W^T \mathcal{Y} A W & W^T \mathcal{Y} B \\ \hline I & 0 \\ C W & D \end{array} \right) \succ 0. \quad (5.50)$$

We transform our nonlinear matrix inequality into a valid LMI form by applying congruence transformation result (5.50) to inequality (5.37) and changing variables such as

$$\mathbf{A}_C^T := -Y \mathcal{A}^T + C_C^T \mathcal{B}_u^T - A_C^T (\hat{X} - Y), \quad (5.51)$$

$$\mathbf{B}_C^T := B_C^T (\hat{X} - Y), \quad (5.52)$$

$$\mathbf{C}_C^T := C_C^T, \quad (5.53)$$

$$\mathbf{D}_C^T := D_C^T. \quad (5.54)$$

Then, inequalities we need to solve for a stable feedforward controller design with dynamic IQC will be:

$$(\star)^T \left(\begin{array}{cc|c} 0 & I & 0 \\ \hline I & 0 & 0 \\ \hline 0 & 0 & M \end{array} \right)$$

$$\times \begin{pmatrix} -\hat{X}\mathcal{A}^T & -\hat{X}\mathcal{A}^T & -\hat{X}\mathcal{C}^T \\ \mathbf{A}_C^T & -Y\mathcal{A}^T - \mathbf{C}_C^T\mathcal{B}_u^T & -Y\mathcal{C}^T - \mathbf{C}_C^T\mathcal{D}_u^T \\ \hline I & 0 & 0 \\ 0 & I & 0 \\ \hline -\mathcal{B}_\phi^T & -\mathcal{B}_\phi^T & -\mathcal{D}_\phi^T \\ 0 & 0 & -\mathcal{D}_p^T \\ -\mathcal{B}_w^T - \mathbf{D}_C^T\mathcal{B}_u^T - \mathbf{B}_C^T & -\mathcal{B}_w^T - \mathbf{D}_C^T\mathcal{B}_u^T & -\mathcal{D}_w^T - \mathbf{D}_C^T\mathcal{D}_u^T \end{pmatrix} \succ 0, \quad (5.55)$$

$$T^T\hat{X}T - \begin{pmatrix} X & 0 \\ 0 & 0 \end{pmatrix} \succ 0 \quad (5.56)$$

and

$$Y - \hat{X} \succ 0. \quad (5.57)$$

Then, if we apply Schur complement formula (4.6) to inequality (5.55) we obtain feasible LMIs which can be solved using YALMIP and SEDUMI. We solve for \mathbf{A}_C , \mathbf{B}_C , \mathbf{C}_C and \mathbf{D}_C while minimizing γ then we convert them to our actual state matrices A_C , B_C , C_C and D_C . C_{ff} is constructed using this state matrices of controller.

5.3.3. Selection of Multipliers

For our problem, we have 2 uncertain parameters c_F and v since we define $c_R = c_F$ and uncertainty block is in the form of

$$\Delta = \begin{pmatrix} \delta_{c_F}I & 0 \\ 0 & \delta_v I \end{pmatrix} = \begin{pmatrix} \Delta_1 & 0 \\ 0 & \Delta_2 \end{pmatrix}. \quad (5.58)$$

Then, form of Θ will be

$$\Theta = \left(\begin{array}{c|c} \Theta_{11} & \Theta_{12} \\ \hline \Theta_{12}^* & \Theta_{22} \end{array} \right) = \left(\begin{array}{cc|cc} \Theta_{11}^1 & 0 & \Theta_{12}^1 & 0 \\ 0 & \Theta_{11}^2 & 0 & \Theta_{12}^2 \\ \hline \star & 0 & \Theta_{22}^1 & 0 \\ 0 & \star & 0 & \Theta_{22}^2 \end{array} \right) \quad (5.59)$$

As discussed in [19], since c_F and v are real-valued constant uncertainties, we describe uncertainties with multipliers of the form

$$\phi N \phi^* = \left(\begin{array}{cc} S(j\omega) & 0 \\ 0 & S(j\omega) \end{array} \right) \left(\begin{array}{cc} N_{11} & N_{12} \\ N_{21} & N_{22} \end{array} \right) \left(\begin{array}{cc} S(j\omega) & 0 \\ 0 & S(j\omega) \end{array} \right)^* \quad (5.60)$$

with

$$S(s) = \left(1 \quad \frac{s-p}{s+p} \quad \dots \quad \left(\frac{s-p}{s+p} \right)^{n_s} \right) \otimes I. \quad (5.61)$$

and static part N is chosen in different structures and compared for selection of best form for our problem. One is chosen as discussed in [10] in the form of

$$N = \left(\begin{array}{cc} N_{11} & N_{12} \\ N_{21} & N_{22} \end{array} \right) = \left(\begin{array}{cc} Q & K \\ K^T & R \end{array} \right) \quad (5.62)$$

where $K = -K^*$ (skew-symmetric). Also one multiplier is chosen as discussed in [9] in the form of

$$N = \left(\begin{array}{cc} N_{11} & N_{12} \\ N_{21} & N_{22} \end{array} \right) = \left(\begin{array}{cc} V & K \\ K^* & -V \end{array} \right). \quad (5.63)$$

For our problem, we have 2 uncertain parameters c_F and v since we define $c_R = c_F$ and uncertainty block is in the form of 5.58. We choose V according to this Δ in the

form of

$$V = \begin{pmatrix} V_1 & 0 \\ 0 & V_2 \end{pmatrix} \quad (5.64)$$

and we choose K in the form of

$$K = \begin{pmatrix} K_1 & 0 \\ 0 & K_2 \end{pmatrix}. \quad (5.65)$$

We can easily show that such a multiplier meet our requirements as follows:

$$\begin{pmatrix} I \\ \delta I \end{pmatrix}^T \begin{pmatrix} V & K \\ K^* & -V \end{pmatrix} \begin{pmatrix} I \\ \delta I \end{pmatrix} = \begin{pmatrix} I & \delta I \end{pmatrix} \begin{pmatrix} V + \delta K \\ K^* - \delta V \end{pmatrix} \quad (5.66)$$

$$= V + \delta K + \delta K^* - \delta^2 V \quad (5.67)$$

$$= V + \delta \underbrace{(K + K^*)}_0 - \delta^2 V \quad (5.68)$$

$$= V - \delta^2 V \quad (5.69)$$

$$= \underbrace{V}_{>0} \underbrace{(1 - \delta^2)}_{\geq 0} \succeq 0. \quad (5.70)$$

5.3.4. Generating LMIs for Static Multipliers

For the close loop system (3.45), our objective is to hold following inequality for performance and robustness with suitable multipliers such as

$$\begin{pmatrix} I \\ -G_{cl}^* \end{pmatrix}^* M \begin{pmatrix} I \\ -G_{cl}^* \end{pmatrix} \succ 0 \quad (5.71)$$

where

$$\begin{pmatrix} I \\ -G_{cl}^* \end{pmatrix} = \left[\begin{array}{cc|cc} -A^T & 0 & -C_q^T & -C_z^T \\ -C_C^T B_u^T & -A_C^T & -C_C^T D_{qu}^T & -C_C^T D_{zu}^T \\ \hline 0 & 0 & I & 0 \\ -B_p^T & 0 & -D_{qp}^T & -D_{zp}^T \\ 0 & 0 & 0 & I \\ -B_w^T - D_C^T B_u^T & -B_C^T & -D_{qw}^T - D_C^T D_{qu}^T & -D_{zw}^T - D_C^T D_{zu}^T \end{array} \right] \quad (5.72)$$

and

$$M = \begin{pmatrix} N_{11} & N_{12} & 0 & 0 \\ N_{21} & N_{22} & 0 & 0 \\ 0 & 0 & \gamma I & 0 \\ 0 & 0 & 0 & -\gamma^{-1} \end{pmatrix}. \quad (5.73)$$

But we need to put it in a numerically solvable LMI form since we cannot solve it for all frequencies. KYP lemma is used to convert frequency dependent matrix inequalities to feasible LMIs. Applying KYP lemma to (5.72) we obtain the following inequality.

If $\exists \mathcal{Y} = \mathcal{Y}^T$ such that

$$(\star)^T \begin{pmatrix} 0 & \mathcal{Y} & 0 \\ \mathcal{Y} & 0 & 0 \\ 0 & 0 & M \end{pmatrix}$$

$$\times \underbrace{\begin{pmatrix} -A^T & 0 & -C_q^T & -C_z^T \\ -C_C^T B_u^T & -A_C^T & -C_C^T D_{qu}^T & -C_C^T D_{zu}^T \\ \hline I & 0 & 0 & 0 \\ 0 & I & 0 & 0 \\ \hline 0 & 0 & I & 0 \\ -B_p^T & 0 & -D_{qp}^T & -D_{zp}^T \\ 0 & 0 & 0 & I \\ -B_w^T - D_C^T B_u^T & -B_C^T & -D_{qw}^T - D_C^T D_{qu}^T & -D_{zw}^T - D_C^T D_{zu}^T \end{pmatrix}}_{\begin{pmatrix} A & B \\ I & 0 \\ \hline C & D \end{pmatrix}} \succ 0, \quad (5.74)$$

then stability is guaranteed and \mathcal{L}_2 -gain of performance channel is robustly smaller than γ .

Then we repeat equations (5.46 - 5.50) to $\begin{pmatrix} I \\ -G_{cl}^* \end{pmatrix}$ to obtain LMIs for static IQCs. It can be considered as a similar procedure applied to dynamic multiplier for another system $\begin{pmatrix} I \\ -G_{cl}^* \end{pmatrix}$.

Different than dynamic multipliers, we only want

$$\mathcal{Y} = \begin{pmatrix} Y & I \\ \hline I & (Y - \hat{X})^{-1} \end{pmatrix} \succ 0 \quad (5.75)$$

since there is no dynamic part of multipliers to couple with main inequality. With respect to the ‘Schur Complement’ formula, this is equivalent to

$$Y - (Y - \hat{X}) \succ 0 \text{ and } (Y - \hat{X})^{-1} \succ 0. \quad (5.76)$$

We can equivalently write

$$\hat{X} \succ 0 \text{ and } Y - \hat{X} \succ 0. \quad (5.77)$$

Then, inequalities we need to solve for a stable feedforward controller design with static IQC will be:

$$\begin{aligned}
 & (\star)^T \begin{pmatrix} 0 & I & 0 \\ I & 0 & 0 \\ 0 & 0 & M \end{pmatrix} \\
 & \begin{pmatrix} -\hat{X}A^T & -\hat{X}A^T & -\hat{X}C_q^T & -\hat{X}C_z^T \\ \mathbf{A}_C^T & -YA^T - \mathbf{C}_C^T B_u^T & -YC_q^T - \mathbf{C}_C^T D_{qu}^T & -YC_z^T - \mathbf{C}_C^T D_{zu}^T \\ I & 0 & 0 & 0 \\ 0 & I & 0 & 0 \\ 0 & 0 & I & 0 \\ 0 & 0 & 0 & I \\ -B_p^T & -B_p^T & -D_{qp}^T & -D_{zp}^T \\ -B_w^T - \mathbf{D}_C^T B_u^T - \mathbf{B}_C^T & -B_w^T - \mathbf{D}_C^T B_u^T & -D_{qw}^T - \mathbf{D}_C^T D_{qu}^T & -D_{zw}^T - \mathbf{D}_C^T D_{zu}^T \end{pmatrix} \succ 0, \quad (5.78)
 \end{aligned}$$

$$\hat{X} \succ 0. \quad (5.79)$$

$$Y - \hat{X} \succ 0. \quad (5.80)$$

Then, if we apply the ‘Schur Complement’ formula to inequality (5.78) we obtain feasible LMIs which can be solved using YALMIP and SEDUMI. We solve for \mathbf{A}_C , \mathbf{B}_C , \mathbf{C}_C and \mathbf{D}_C while minimizing γ then we convert them to our actual A_C , B_C , C_C , D_C . C_{ff} is constructed using this state matrices of controller same as the dynamic multipliers.

6. FEEDFORWARD CONTROLLER SYNTHESIS USING IQCS

In this chapter, using the theory explained in Chapter 5, feedforward controller is designed to work with feedback controller. Two different feedforward controller is designed. One is using static multipliers and other is using dynamic multiplier with the dual IQCs. In order to obtain optimum controller we solve LMIs built for static and dynamic multipliers using YALMIP as parser and SEDUMI as solver.

6.1. Controller Synthesis

We design different feedforward controller using both dynamic and static IQCs. Static and dynamic parts of multipliers can be chosen in different structures. A list of IQCs is given in [9] and [10] which are used to design our controllers. Yaw rate tracking of our model for step input is also presented to compare classical feedback control response and feedforward controllers affects. We also compare different feedforward controllers designed with multipliers in different forms.

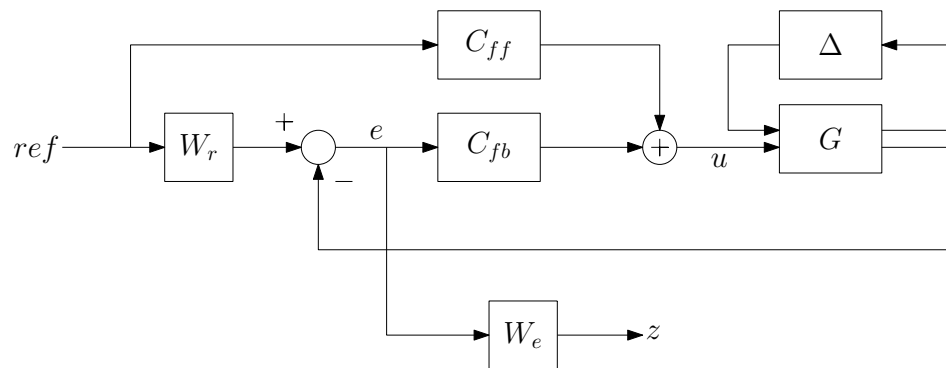


Figure 6.1. System interconnection for FF controller design.

6.1.1. Selection of the Weighting Functions

Selection of weights is important for H_∞ controller design. It is difficult to find suitable weight function for both stability and performance requirements. The results

of the design depend on weighting functions for all kind of design method [27].

Input filter W_r has been designed as a second order Butterworth filter with a cut-off frequency of $2Hz$ considering upper limit of driver activity which is

$$W_r(s) = \frac{157.9137}{1.0000s^2 + 17.7715s + 157.9137} \quad (6.1)$$

Output filter W_e has been chosen as an approximate integrator such as

$$W_e(s) = \frac{1}{s + 0.001} \quad (6.2)$$

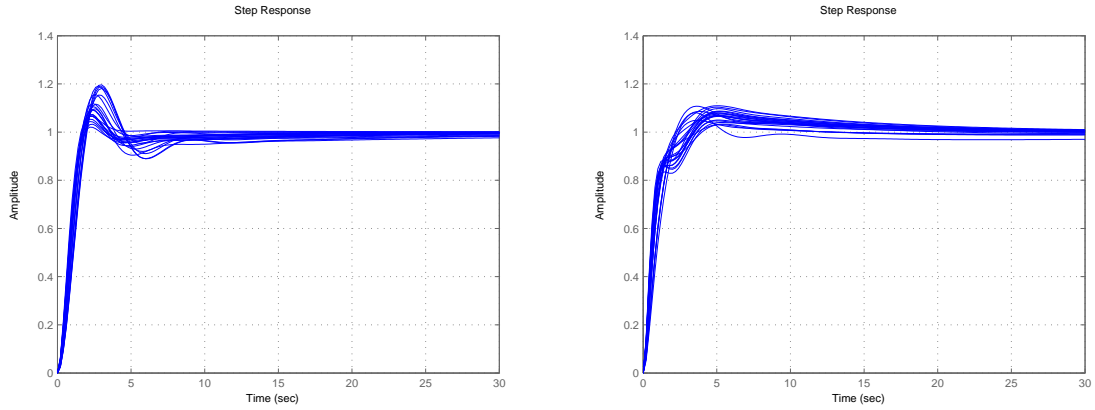
6.1.2. Controller Synthesis with Static Multipliers

Several FF controllers designed with different static multipliers and yaw rate tracking for step input is also presented to compare classical FB control response and affect of FF controller.

6.1.2.1. Static Design 1. If we choose multiplier with zero off-diagonal terms such as;

$$N = \begin{pmatrix} N_{11} & N_{12} \\ N_{21} & N_{22} \end{pmatrix} = \begin{pmatrix} V & 0 \\ 0 & -V \end{pmatrix}, V \succ 0 \quad (6.3)$$

which is in the form discussed in [9] and solve the inequality with this multiplier, we obtain a feedforward controller which improve the yaw rate tracking performance of vehicle as seen in Figure 6.2.



(a) Feedback

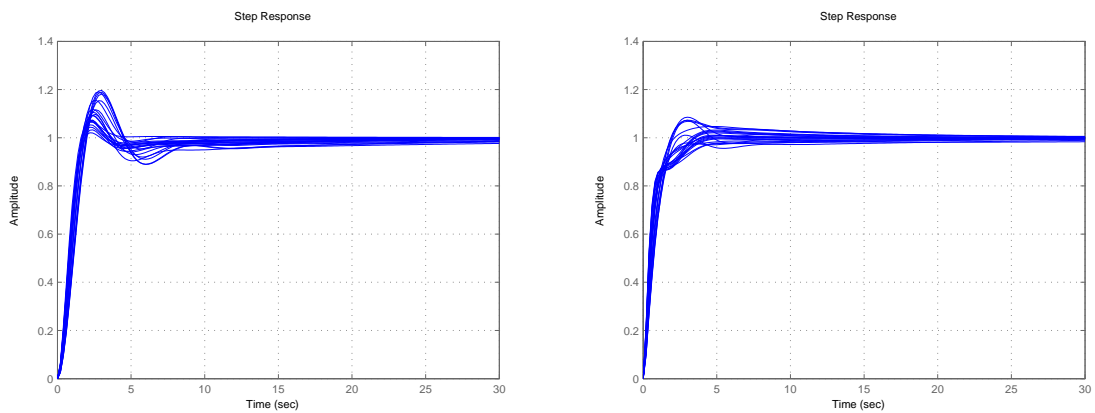
(b) Feedforward

Figure 6.2. Step response of system with static design 1.

6.1.2.2. Static Design 2. If we select off-diagonal terms of multiplier skew symmetric such as;

$$N = \begin{pmatrix} N_{11} & N_{12} \\ N_{21} & N_{22} \end{pmatrix} = \begin{pmatrix} V & K \\ K^T & -V \end{pmatrix} \quad (6.4)$$

where K is skew symmetric and $V \succ 0$, then designed controller improve robustness more then design made with multiplier with zero off-diagonal terms. But there is still overshoot and uncertainty band is large.



(a) Feedback

(b) Feedforward

Figure 6.3. Step response of system with static design 2.

6.1.3. Controller Synthesis with Dynamic Multipliers

We separate dynamic parts and static parts of multiplier as discussed before. Dynamic parts is chosen as in (5.61) and forms of static parts are also used in this section. They are combined with dynamic part as shown in (5.60) in the form of $\phi N \phi^*$

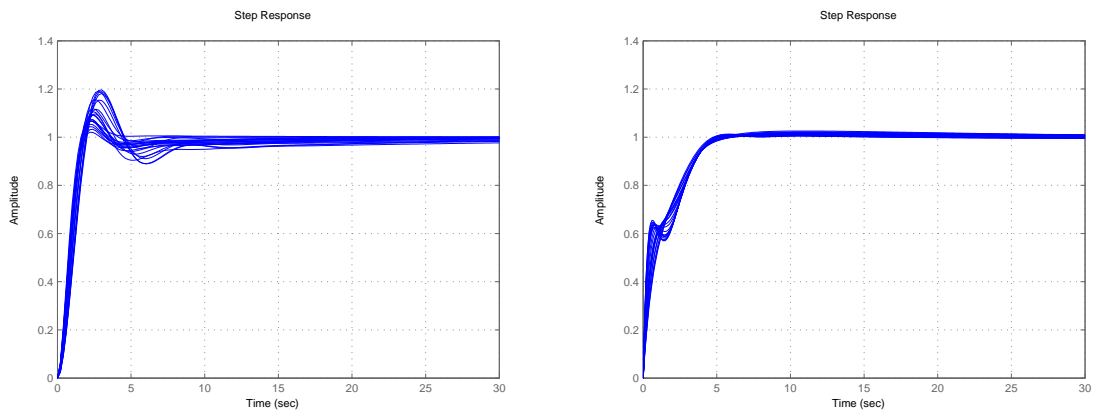
6.1.3.1. Dynamic Design 1. If we choose $n_s = 1$ and $p = 1$ then $S(s)$ will be

$$S(s) = \begin{pmatrix} 1 & \frac{s-1}{s+1} \end{pmatrix} \otimes I \quad (6.5)$$

and static part of multiplier as;

$$N = \begin{pmatrix} N_{11} & N_{12} \\ N_{21} & N_{22} \end{pmatrix} = \begin{pmatrix} V & 0 \\ 0 & -V \end{pmatrix}, V \succ 0 \quad (6.6)$$

and solve the inequality, we obtain improvement of robustness and performance comparing to design made with static multipliers. There is no overshoot and uncertainty band is very narrow.



(a) Feedback

(b) Feedforward

Figure 6.4. Step response of system with dynamic design 1.

6.1.3.2. Dynamic Design 2. If we change $n_s = 2$ then $S(s)$ will be

$$S(s) = \left(1 \quad \frac{s-1}{s+1} \quad \left(\frac{s-1}{s+1}\right)^2 \right) \otimes I \quad (6.7)$$

and solve the inequality again, we don't obtain better result than the design with $n_s = 1$.

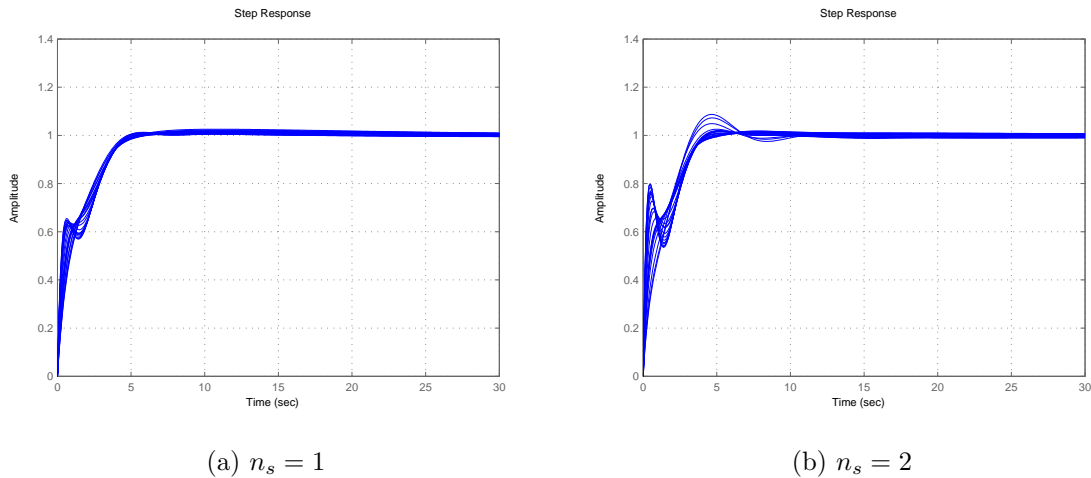


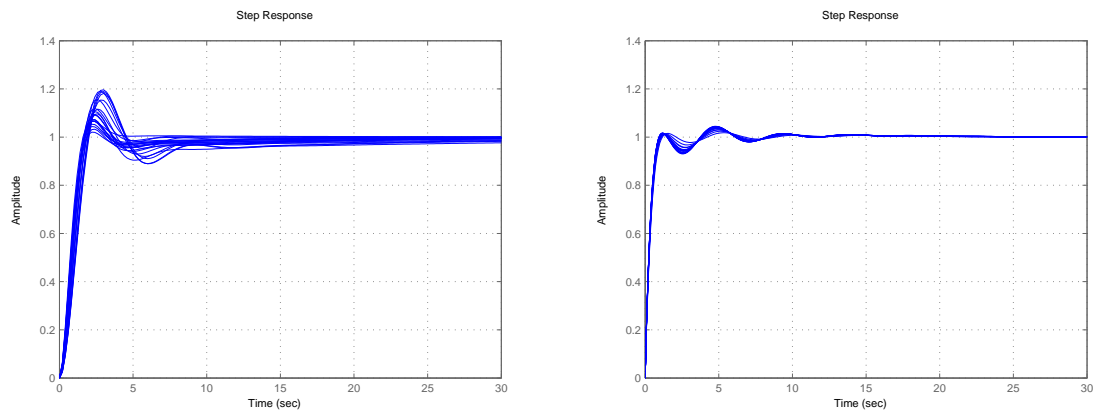
Figure 6.5. Step response of system with dynamic design 2.

6.1.3.3. Dynamic Design 3. If we select off-diagonal terms of static part skew symmetric as discussed in [19] and choose V in the form of (5.64) such that

$$N = \begin{pmatrix} N_{11} & N_{12} \\ N_{21} & N_{22} \end{pmatrix} = \begin{pmatrix} V & K \\ K^T & -V \end{pmatrix} \quad (6.8)$$

where K is skew symmetric and $V \succ 0$, then rising time decrease significantly as seen in following figure. Even there is some overshoot and fluctuations, it would be preferred considering rising time.

In this chapter, we design several feedforward controller using static and dynamic multipliers. It is seen that design made with dynamic multipliers have better yaw rate tracking performance and robustness comparing to ones made with static multipliers. There are two good dynamic design. One is using multiplier which have dynamic



(a) Feedback

(b) Feedforward

Figure 6.6. Step response of system with dynamic design 3.

part build with $n_s = 1$ and $p = 1$ and static part is $\begin{pmatrix} V & 0 \\ 0 & -V \end{pmatrix}$ and other is using multiplier which static part is $\begin{pmatrix} V & K \\ K^T & -V \end{pmatrix}$. The one with skew symmetric off-diagonal terms can be used for our design considering its rising time but the first one deal with uncertainties better. In the following chapter, we give the comparison of yaw rate and beta tracking performance of them and also give response for several driving conditions.

7. SIMULATIONS

In road, driver give a wheel angle with experience and vehicle respond to that input depending on speed of the vehicle and road characteristic if we assume other parameters are constant on operation. In this chapter, we explain calculation of reference values corresponding to drivers command and we give simulation results for different drivers input. Finally, we give simulation result of real road data collecting by a manufacturer of data acquisition equipment for vehicles.

7.1. Reference Values Corresponding to Drivers Steering Input

We designed controllers to track reference yaw rate while trying to keep sideslip angle as low as possible with a desirable upper limit. It is required to create reference yaw rate and sideslip angle values corresponding to drivers steering input. Yaw rate and sideslip angle are two states of linear single track model. Reference yaw rate and sideslip angle values corresponding to drivers steering input is constructed based on steady state response of linear single track model as explained in [4] and [28].

Steady state responses of linear single track for beta and yaw rate are.

$$\beta_{ss}(t) = -\frac{C_F C_R L_R (L_F + L_R) - L_F m C_F v^2}{C_F C_R (L_F + L_R)^2 + m v^2 (L_R C_R - L_F C_F)} \quad (7.1)$$

and

$$\dot{\psi}_{ss}(t) = -\frac{C_F C_R (L_F + L_R) v}{C_F C_R (L_F + L_R)^2 + m v^2 (L_R C_R - L_F C_F)}. \quad (7.2)$$

These references are saturated by $\beta_{max} = 2^\circ$ and $\dot{\psi}_{max} = \mu g / v$ [2]. Then reference yaw rate and beta become

$$\beta_{ref}(t) = \min \{ \beta_{ss}(t), 2^\circ \text{sign}(\beta) \} \quad (7.3)$$

and

$$\dot{\psi}_{ref}(t) = \min \left\{ \dot{\psi}_{ss}(t), \frac{\mu g}{v} \text{sign}(\psi) \right\}. \quad (7.4)$$

7.2. Lane Change Maneuver

A Lane change maneuver is an important issue for lateral vehicle dynamic control and we want to see behavior of our controller for following such a desired trajectory. Following figure is obtained in [29] and we use this to create our simulation signal for lane change.

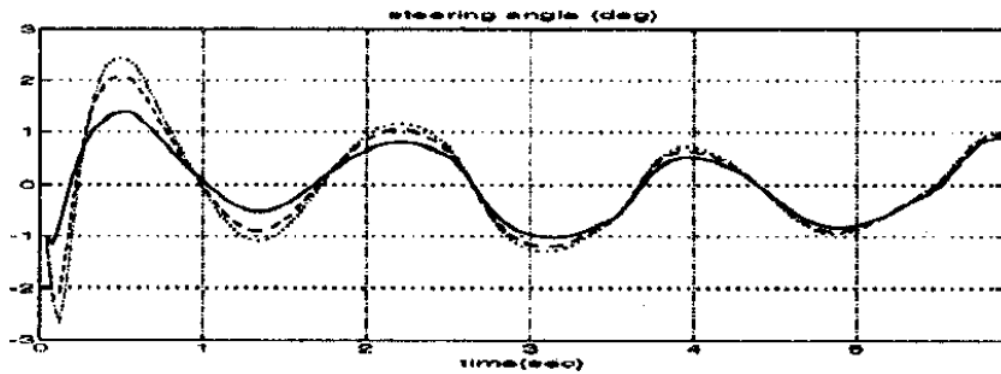


Figure 7.1. Steering angle of lane change maneuver [29].

As seen in Figure 7.1 and discussed also in [30] we can use sinusoidal signals for simulate lane change maneuvers.

7.3. Fishhook Maneuver

The fishhook maneuver is steering reversal at maximum vehicle roll angle to measure rollover resistance [31]. It is also useful maneuver for yaw rate tracking since yaw rate is also at maximum level in both direction. Even if we do not consider roll dynamic in this study, it would be helpful to see behavior of designed controller with maximum yaw rate limits.

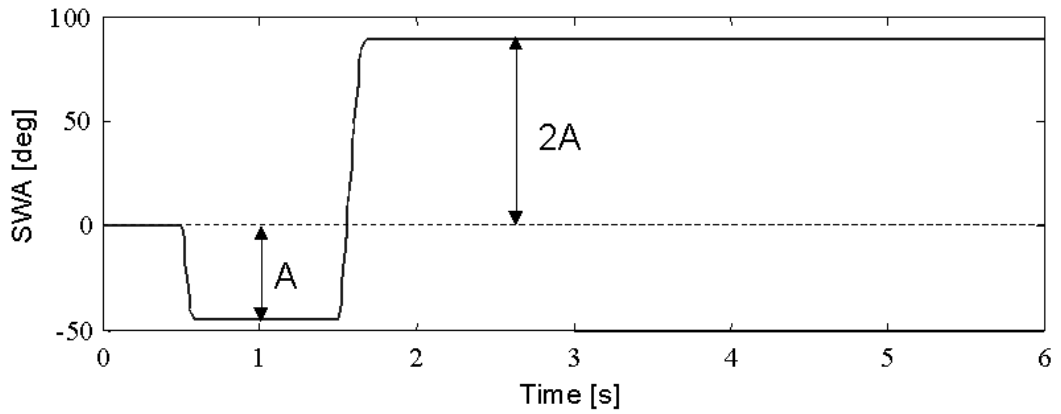


Figure 7.2. Fishhook maneuver steering wheel angle [31].

7.4. Simulation Results

Figures 7.3-7.5 show tracking response of controlled system for different values of parameters in order to see behavior of both FB and FF controllers with the change of uncertain parameters. 5 points sampled in the range of uncertainties which are $(40kN - 80kN)$ for cornering stiffness and $(36km/h - 108km/h)$ for vehicle speed.

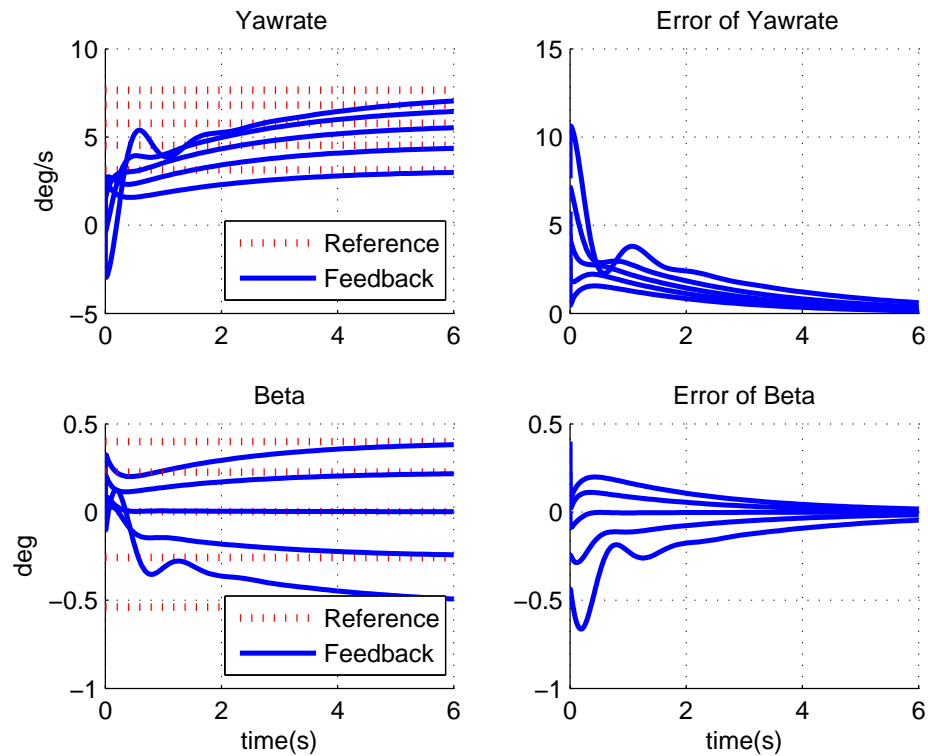


Figure 7.3. Response of vehicle with FB controller.

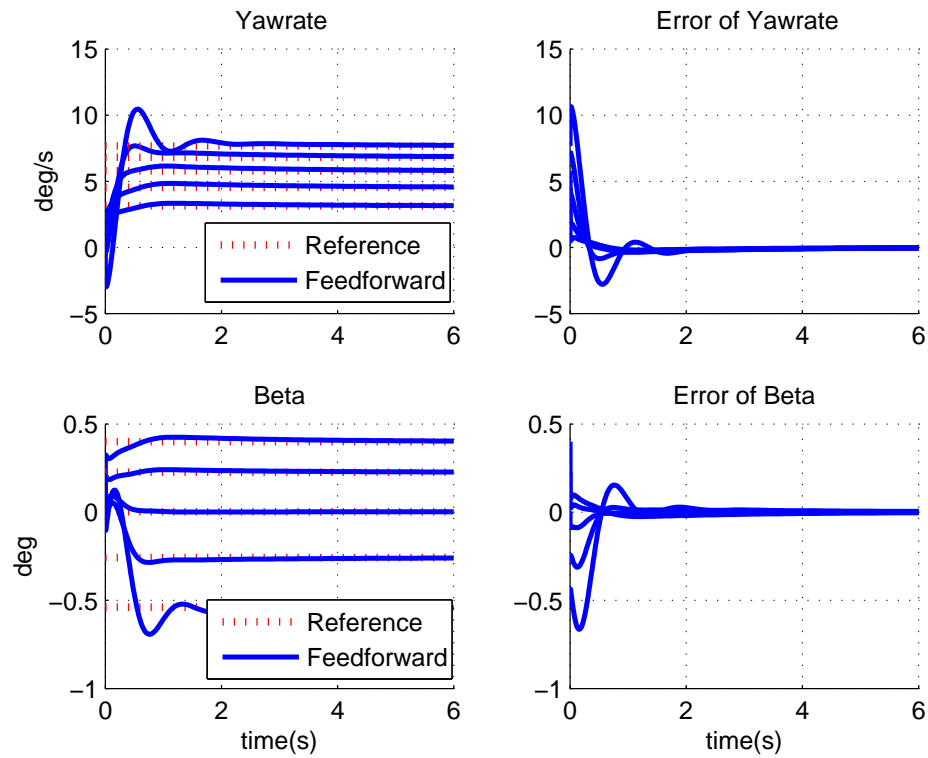


Figure 7.4. Response of vehicle with FB/FF controller designed with static IQCs.

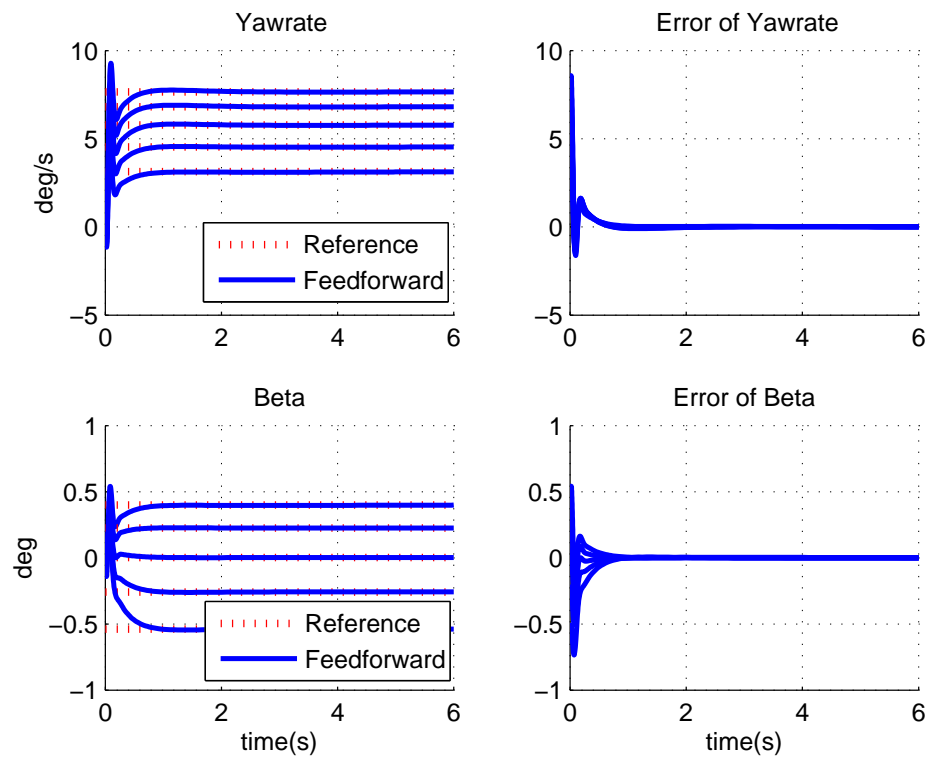


Figure 7.5. Response of vehicle with FB/FF controller designed with dynamic IQCs.

It is seen that Static FB/FF design responds better than FB, and Dynamic FB/FF design responds better than Static FB/FF design. It is clearly seen in Figure 7.5 that Dynamic design is more robust and have better performance. Figures 7.7-7.13 show comparison of Dynamic FB/FF design with FB only simulations. Tracking performance of sinusoidal steering inputs are given to simulate lane change maneuver in Figures 7.7-7.8. Fishhook maneuver is also given in Figure 7.12. We simulate our system for steering angles collected from a real vehicle with 172 km/h average speed and yaw rate tracking results are compared with feedback in 7.13. We also give simulation results of random steering angle with 1deg. mean to simulate cornering with small steering angle in Figures 7.10-7.11.

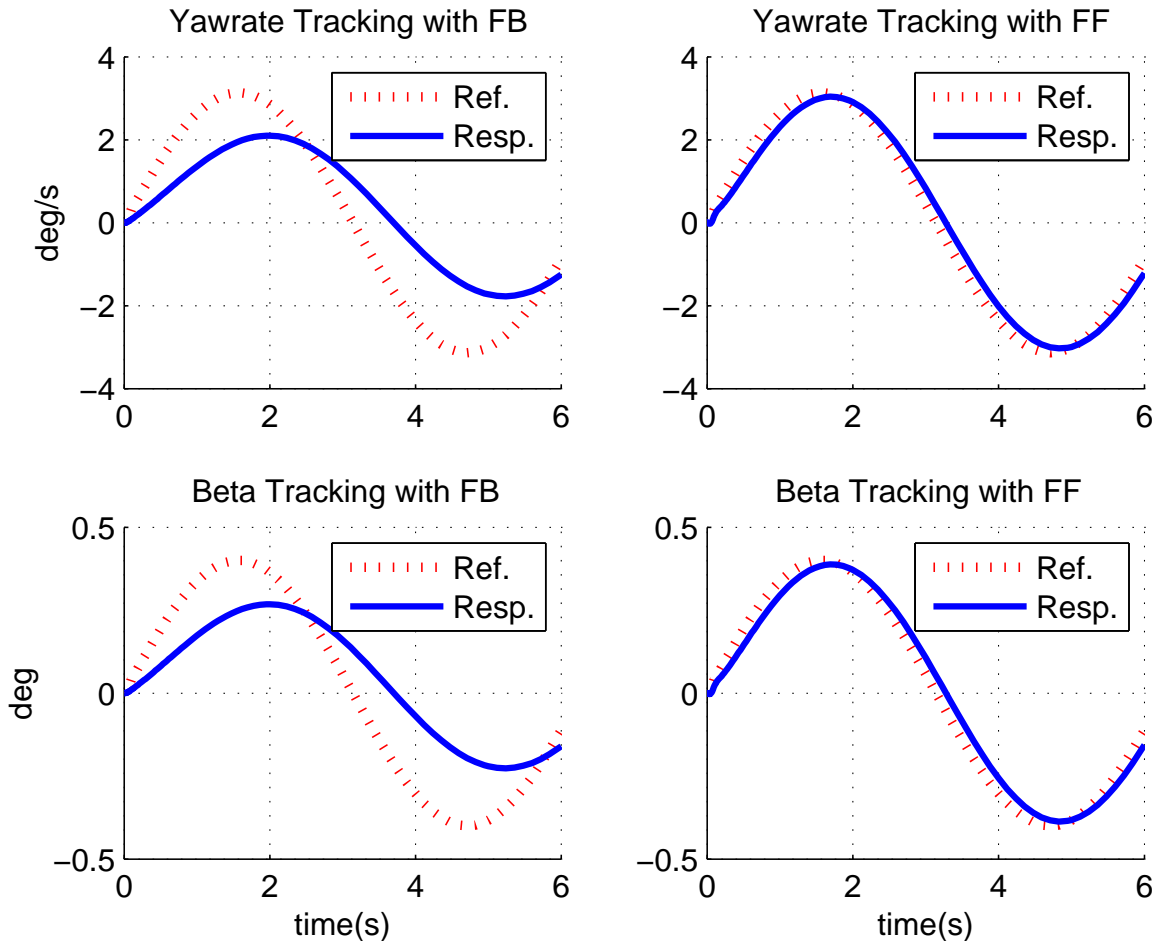


Figure 7.6. Sinusoidal steering input for $v = 36\text{km/h}$.

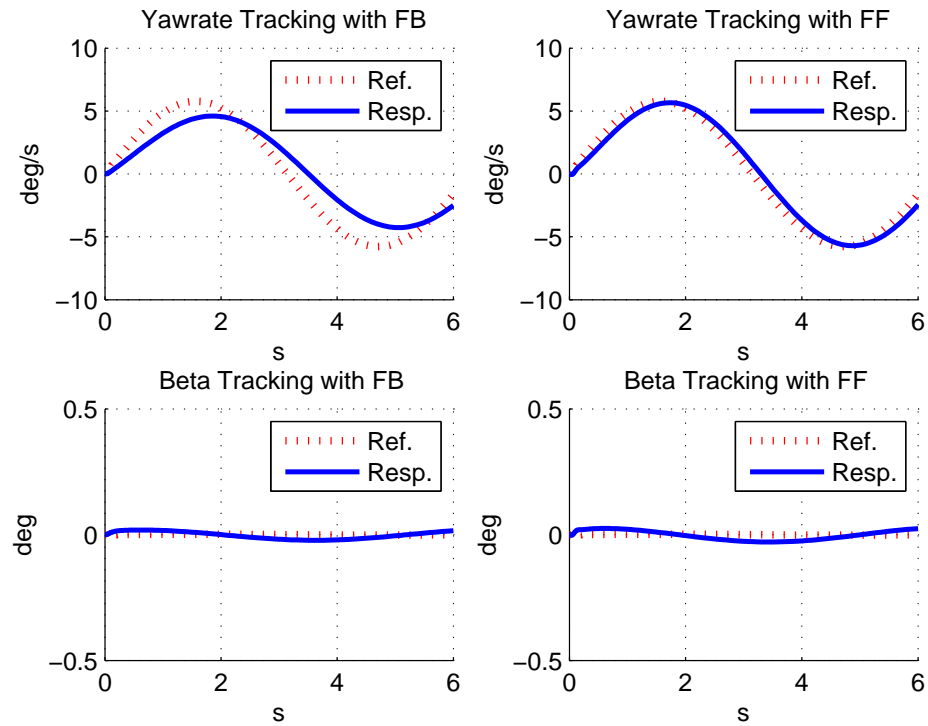


Figure 7.7. Sinusoidal steering input for $v = 72 \text{ km/h}$.

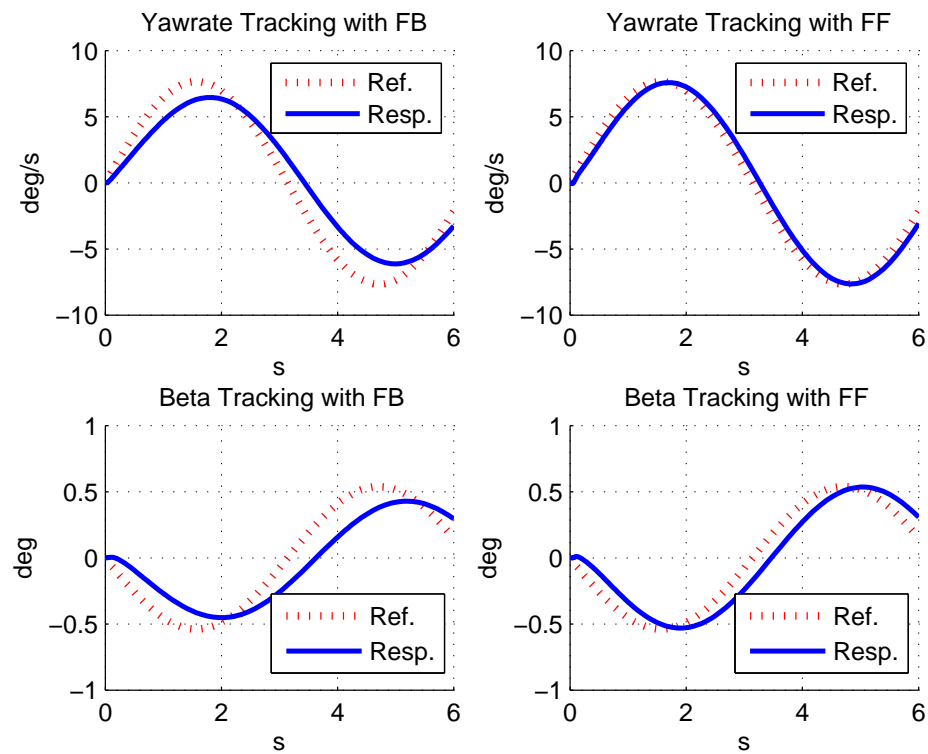


Figure 7.8. Sinusoidal steering input for $v = 108 \text{ km/h}$.

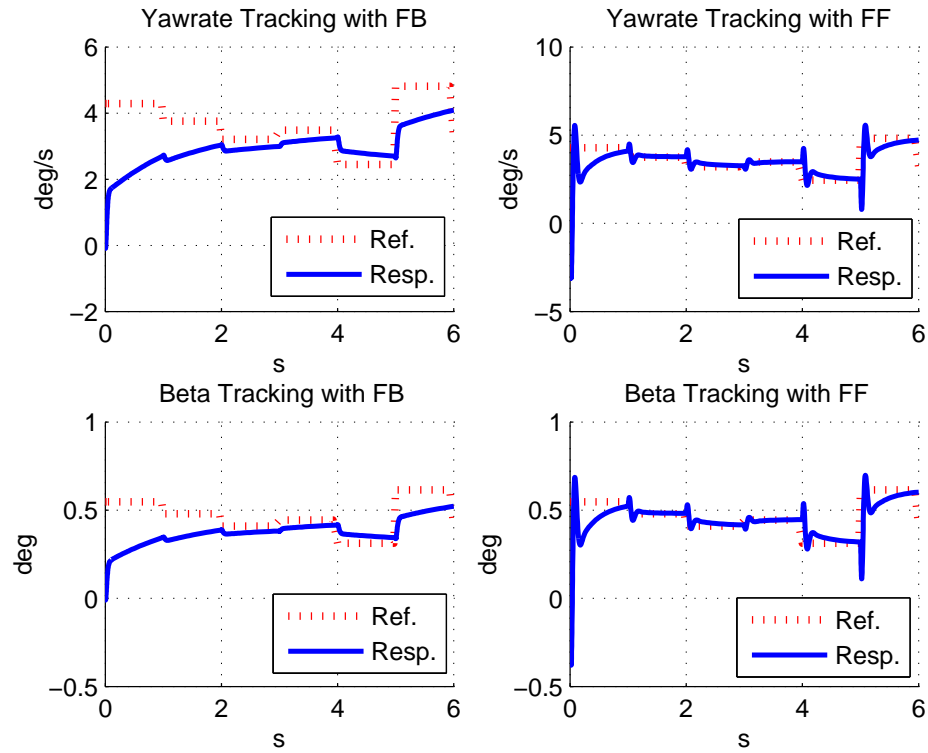


Figure 7.9. Random steering input with 1 degree mean for $v = 36\text{km/h}$.

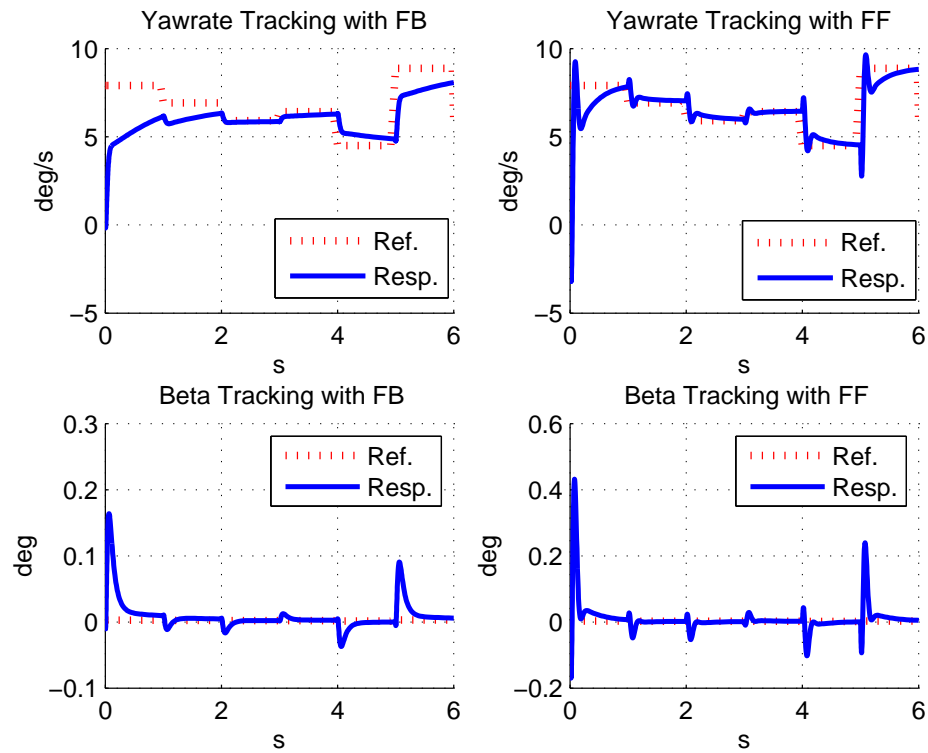


Figure 7.10. Random steering input with 1 degree mean for $v = 72\text{km/h}$.

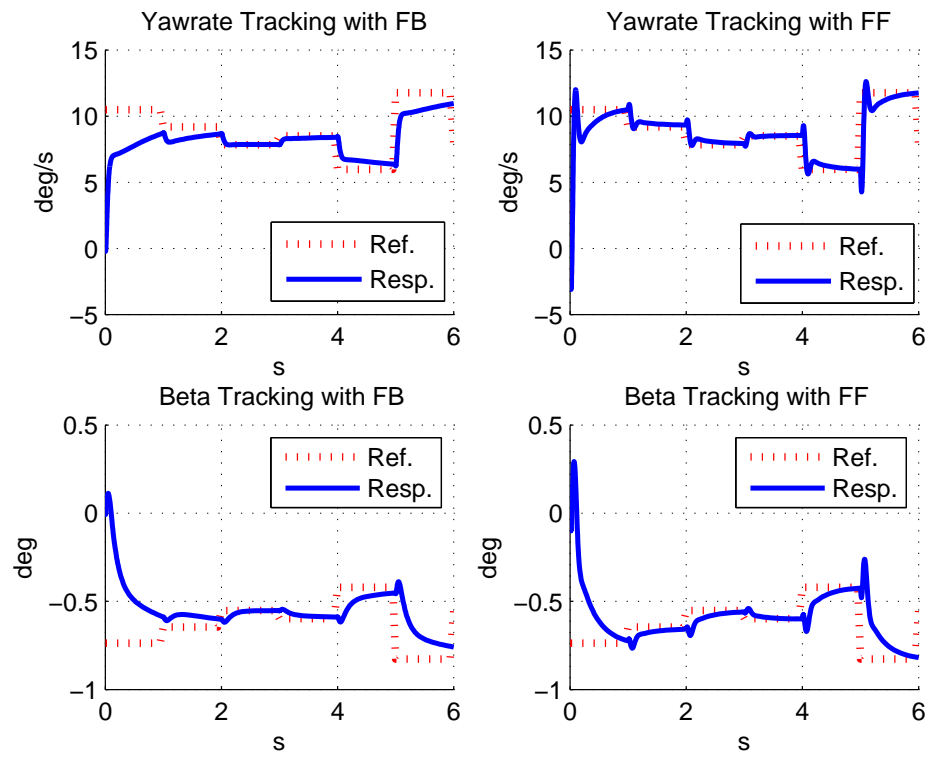


Figure 7.11. Random steering input with 1 degree mean for $v = 108\text{km/h}$.

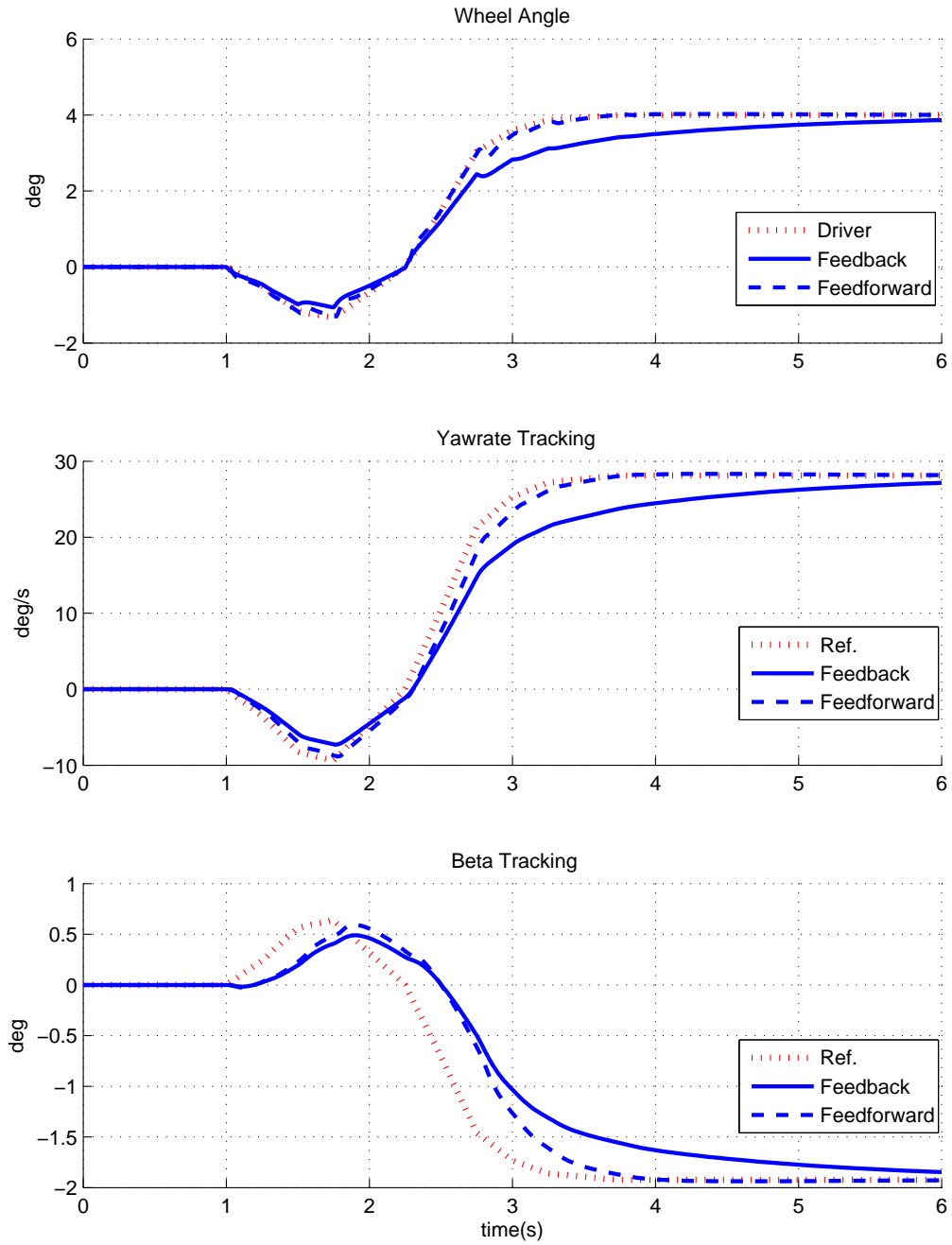


Figure 7.12. Fishhook maneuver for $v = 108\text{km/h}$.

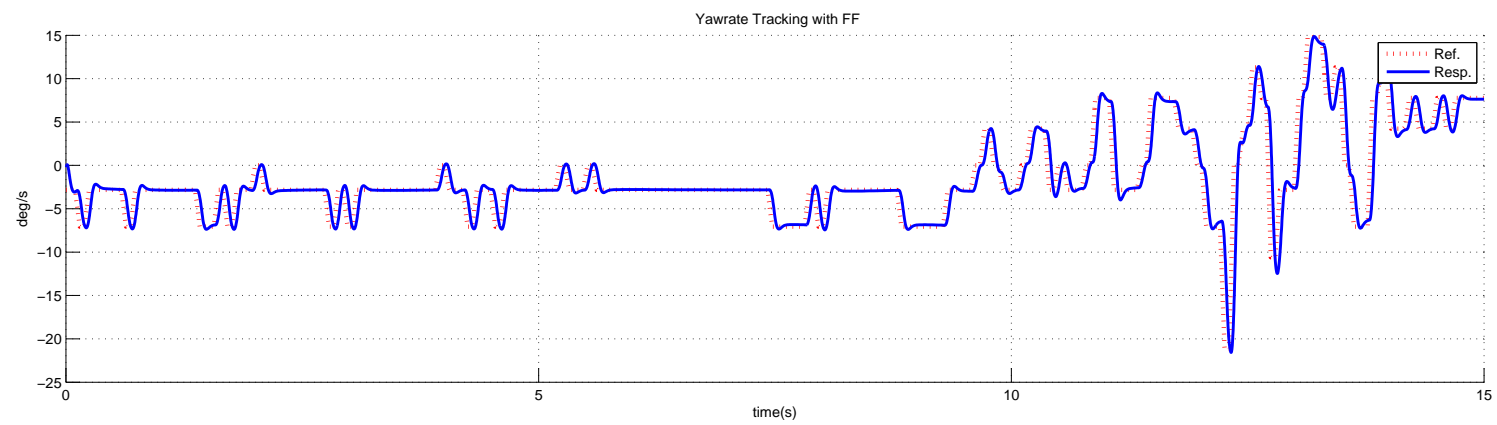
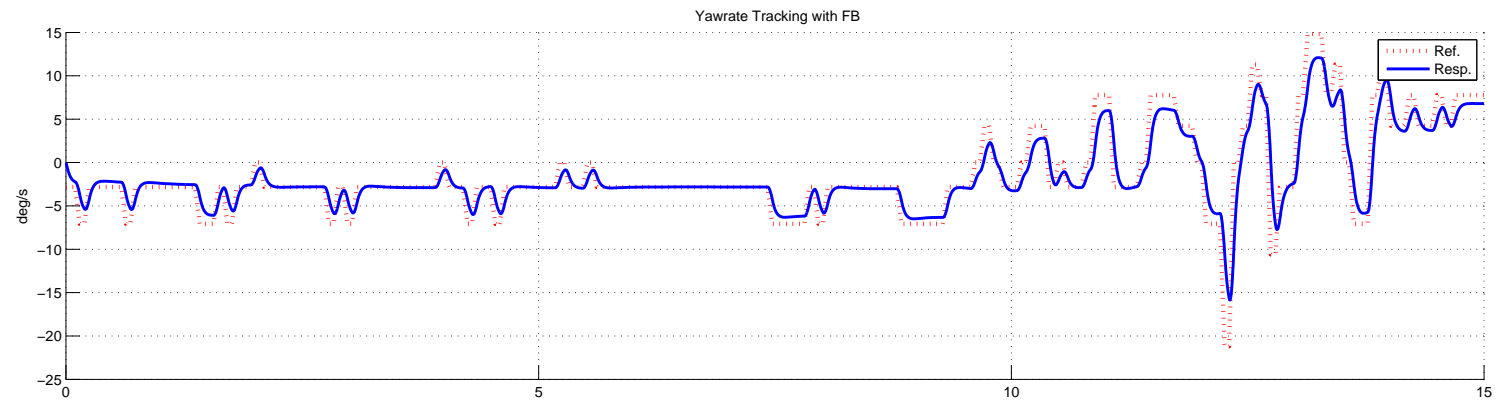


Figure 7.13. Real steering angle data for $v = 172km/h$ average.

8. CONCLUSIONS

We design a robust feedforward controller for active steering using results of [9], [10] and [26]. Feedforward controller is designed and used with feedback controller to improve robustness and performance since the feedback controller cannot show sufficient tracking performance even for small changes of uncertain parameters.

A PID feedback controller is designed to stabilize a linear single track vehicle model with optimization of PID parameters and feedforward controller is added to this controlled system to deal with uncertainties such as speed and cornering stiffness. Linear parameter varying (LPV) control theory and stability analysis results of integral quadratic constraints (IQCs) are used for the synthesis of feedforward controller. Both static and dynamic IQCs are used to describe uncertainty of the system and dual IQCs are used for analysis because of the nature of feedforward problem. Linear matrix inequalities (LMIs) are used to define stability conditions.

It is seen that Static FB/FF design responds better than FB, and Dynamic FB/FF design responds better than Static FB/FF design. But computational cost of feedforward controller designed with dynamic multipliers is high. We can only solve the problem for several uncertain parameters and range of the uncertainties is smaller comparing to design using static multiplier. However design using static IQCs are faster and we can consider uncertainties in more parameters and we can obtain results for larger uncertainty ranges. But robustness of controller designed with static IQCs is not as good as the one with dynamic IQCs. So we should specify exactly which uncertainties are affecting robustness more for dynamic design.

Simulation results of feedback controller, feedforward controller designed with static IQCs and feedforward controller designed with dynamic IQCs are given and compared for different steering angles.

Only lateral vehicle dynamic control is considered in this study. Drivers usually overestimate vehicle's roll stability and it increase roll over risk. We can also include roll dynamic for vehicle rollover protection.

Finally, feedforward control design with gain scheduling can be studied to improve active steering. It is possible to measure uncertain parameters during operation for gain scheduling. We can schedule controller using this online measurements using a scheduling function. Although it is not easy to estimate cornering stiffness online, we can at least measure speed and mass, and use for gain scheduling as a future work.

REFERENCES

1. Rajamani, R., *Vehicle Dynamics And Control*, Springer, 2006.
2. Van Zanten, A., “Bosch ESP Systems: 5 Years of Experience”, *SAE Paper*, Vol. 109, No. 2000-01-1633, pp. 428–436, 2000.
3. Ackermann, J., T. Bünte, W. Sienel, H. Jeebe, and K. Naab, “Driving Safety By Robust Steering Control”, *In Proceedings of International Symposium on Advanced Vehicle Control*, Aachen, Germany, 1996.
4. Dixon, J., *Tires, Suspension and Handling*, SAE Publications, 2nd edition, 1996.
5. Sawase, K. and Y. Sano, “Application of Active Yaw Control to Vehicle Dynamics by Utilizing Driving/Braking Force”, *JSAE Review*, Vol. 20, No. 2, pp. 289–295, 1999.
6. Liebermann, E., K. Meder, J. Schuh, and G. Nenninger, “Safety and Performance Enhancement: The Bosch Electronic Stability Control (ESP)”, *SAE Transactions*, Vol. 2004-21-0060, 2004.
7. Bünte, T., D. Odenthal, B. Aksun-Güvenç, and L. Güvenç, “Robust Vehicle Steering Control Design Based On The Disturbance Observer”, *Annual Reviews in Control*, Vol. 26, No. 1, pp. 139–149, 2002.
8. Mammar, S. and D. Koenig, “Vehicle Handling Improvement by Active Steering”, *Vehicle System Dynamics*, Vol. 38, No. 3, pp. 211–242, 2002.
9. Megretski, A. and A. Rantzer, “System Analysis via Integral Quadratic Constraints”, *Automatic Control, IEEE Transactions on*, Vol. 42, No. 6, pp. 819–830, 1997.
10. Scherer, C. W., “LPV Control and Full Block Multipliers”, *Automatica*, Vol. 37,

- No. 3, pp. 361 – 375, 2001.
11. Köse, I. E. and C. W. Scherer, “Robust \mathcal{L}_2 -Gain Feedforward Control of Uncertain Systems Using Dynamic IQCs”, *International Journal of Robust and Nonlinear Control*, Vol. 19, No. 11, pp. 1224–1247, 2009.
 12. De Gelder, E., M. van de Wal, C. Scherer, C. Hol, and O. Bosgra, “Nominal and Robust Feedforward Design With Time Domain Constraints Applied to a Wafer Stage”, *Journal of Dynamic Systems, Measurement, and Control*, Vol. 128, No. 2, pp. 204–215, 2006.
 13. Devasia, S., “Should Model-Based Inverse Inputs be Used as Feedforward Under Plant Uncertainty?”, *Automatic Control, IEEE Transactions on*, Vol. 47, No. 11, pp. 1865 – 1871, November 2002.
 14. Ray, L., “Nonlinear State and Tire Force Estimation for Advanced Vehicle Control”, *Control Systems Technology, IEEE Transactions on*, Vol. 3, No. 1, pp. 117–124, 1995.
 15. Ray, L., “Nonlinear Tire Force Estimation and Road Friction Identification: Simulation and Experiments”, *Automatica*, Vol. 33, No. 10, pp. 1819–1833, 1997.
 16. Smith, N., “Understanding Parameters Influencing Tire Modeling”, *Formula SAE Platform, Dynamics. Department of Mechanical Engineering, Colorado State University Report*, 2004.
 17. Baffet, G., A. Charara, and D. Lechner, “Estimation of Vehicle Sideslip, Tire Force and Wheel Cornering Stiffness”, *Control Engineering Practice*, Vol. 17, No. 11, pp. 1255–1264, 2009.
 18. Hac, A. and E. Bedner, “Robustness of Sideslip Estimation and Control Algorithms for Vehicle Chassis Control”, *Innovations For Safety: Opportunities And Challenges*, 2007.

19. Scherer, C. and I. Köse, “Robustness with Dynamic IQCs: An Exact State-Space Characterization of Nominal Stability with Applications to Robust Estimation”, *Automatica*, Vol. 44, No. 7, pp. 1666–1675, 2008.
20. Boyd, S. and L. Vandenberghe, *Convex Optimization*, Cambridge Univ Pr, 2004.
21. Scherer, C. and S. Weiland, “Linear Matrix Inequalities in Control”, *Lecture Notes, Dutch Institute for Systems and Control, Delft, The Netherlands*, 2000.
22. Skogestad, S. and I. Postlethwaite, *Multivariable Feedback Control: Analysis and Design*, John Wiley & Sons, 2005.
23. Boyd, S., L. El Ghaoui, E. Feron, and V. Balakrishnan, *Linear Matrix Inequalities in System and Control Theory*, Vol. 15, Society for Industrial Mathematics, 1994.
24. Rantzer, A., “On the Kalman-Yakubovich-Popov Lemma”, *Systems and Control Letters*, Vol. 28, pp. 7–10, June 1996.
25. El Ghaoui, L. and S.-I. Niculescu (editors), *Advances in Linear Matrix Inequality Methods in Control: Advances in Design and Control*, Society for Industrial and Applied Mathematics, Philadelphia, PA, USA, 2000.
26. Köse, I. and C. Scherer, “Robust Feedforward Control of Uncertain Systems Using Dynamic IQCs”, *46th IEEE Conference on Decision and Control*, pp. 2181–2186, December 2007.
27. Hu, J., C. Bohn, and H. R. Wu, “Systematic H_∞ Weighting Function Selection and Its Application to the Real-Time Control of a Vertical Take-Off Aircraft”, *Control Engineering Practice*, Vol. 8, No. 3, pp. 241–252, 2000.
28. Başlamışlı, S. C., I. E. Köse, and G. Anlaş, “Gain-Scheduled Integrated Active Steering and Differential Control for Vehicle Handling Improvement”, *Vehicle System Dynamics*, Vol. 47, pp. 99–119, 2009.

29. Chee, W. and M. Tomizuka, "Lane Change Maneuver of Automobiles for the Intelligent Vehicle and Highway System (IVHS)", *American Control Conference, 1994*, Vol. 3, pp. 3586–3587, IEEE, 1994.
30. Miller, R. J. and G. Srinivasan, "Determination of Lane Change Maneuvers Using Naturalistic Driving Data", *National Highway Traffic Safety Administration*, Vol. 05-0337.
31. Hac, A., "Influence of Active Chassis Systems on Vehicle Propensity to Maneuver-Induced Rollovers", *SAE Transactions*, Vol. 2002-01-0967, 2002.